

Taylor columns and inertial-like waves in a three-dimensional odd viscous liquid

E.Kirkinis[†] and M. Olvera de la Cruz

Department of Materials Science & Engineering, Robert R. McCormick School of Engineering and Applied Science, Northwestern University, Evanston IL 60208 USA
Center for Computation and Theory of Soft Materials, Northwestern University, Evanston IL 60208 USA

(Received xx; revised xx; accepted xx)

Odd viscous liquids are endowed with an intrinsic mechanism that tends to restore a displaced particle back to its original position. Since the odd viscous stress does not dissipate energy, inertial oscillations and inertial-like waves can become prominent in such a liquid. In this article we show that an odd viscous liquid in *three* dimensions gives rise to such axially symmetric waves and also to plane-polarized waves. We tacitly assume that an anisotropy axis giving rise to odd viscous effects has already been established and proceed to investigate the effects of odd viscosity on fluid flow behavior. Numerical simulations of the full Navier-Stokes equations show the existence of inertial-like waves downstream a body that moves slowly along the axis of an odd viscous liquid-filled cylinder. The wavelength of the numerically-determined oscillations agrees well with the developed theoretical framework. When odd viscosity is the dominant effect in steady motions, a modified Taylor-Proudman theorem leads to the existence of Taylor columns inside such a liquid. Formation of the Taylor column can be understood as a consequence of helicity segregation and energy transfer along the cylinder axis at group velocity, by the accompanying inertial waves, whenever the reflection symmetry of the system is lost. A number of Taylor column characteristics known from rigidly-rotating liquids, are recovered here for a *non-rotating* odd viscous liquid. These include counter-rotating swirling liquid flow above and below a body moving slowly along the anisotropy axis. Thus, in steady motions, odd viscosity acts to suppress variations of liquid velocity in a direction parallel to the anisotropy axis, inhibiting vortex stretching and vortex twisting. In unsteady and nonlinear motions odd viscosity enhances the vorticity along the same axis, thus affecting both vortex stretching and vortex twisting.

Key words:

1. Introduction

Avron *et al.* (1995) showed that the viscosity tensor $\eta_{\alpha\beta\gamma\delta}$ of the Cauchy stress of a classical liquid

$$\sigma_{\alpha\beta} = \eta_{\alpha\beta\gamma\delta} V_{\gamma\delta} \quad (1.1)$$

can be decomposed into a symmetric and an antisymmetric part : $\eta_{\alpha\beta\gamma\delta} = \eta_{\alpha\beta\gamma\delta}^S + \eta_{\alpha\beta\gamma\delta}^A$ where

$$\eta_{\alpha\beta\gamma\delta}^S = \eta_{\gamma\delta\alpha\beta}^S \quad \text{and} \quad \eta_{\alpha\beta\gamma\delta}^A = -\eta_{\gamma\delta\alpha\beta}^A, \quad (1.2)$$

[†] Email address for correspondence: kirkinis@northwestern.edu

where $V_{\gamma\delta} = \frac{1}{2} \left(\frac{\partial u_\gamma}{\partial x_\delta} + \frac{\partial u_\delta}{\partial x_\gamma} \right)$ is the rate-of-strain tensor and u_α the liquid velocity. The stress tensor (1.1) based on η^S is dissipative. It results in viscous heating (Landau & Lifshitz 1987, §49) which is a positive-definite quadratic form $\text{tr}(\sigma V) = V_{\alpha\beta} \eta_{\alpha\beta\gamma\delta}^S V_{\gamma\delta} > 0$. η^A does not contribute to viscous heating due to its antisymmetry between the first and the second pairs of indices.

The non-dissipative stress $\eta_{\alpha\beta\gamma\delta}^A V_{\gamma\delta}$ is called the odd viscous (or anomalous) stress tensor and its accompanying coefficients odd or Hall viscosity coefficients. This type of behavior can be induced, for instance, by a magnetic field, giving rise to an *anisotropy axis* along its direction. Avron *et al.* (1995) provided a clear physical interpretation of the odd stress tensor that carries over to classical systems. Compression or dilatation gives rise to shear and vice-versa. Thus, it is easy to show, for instance, that a cylinder rotating about its axis in an odd viscous liquid gives rise to a stress $\sigma_{rr}^o = 2\eta_o\Omega$ directed normal to cylinder surface (Avron 1998; Kirkinis 2023), η_o is the dynamic coefficient of odd viscosity and Ω the constant angular velocity of the cylinder.

The ramifications of odd viscosity in classical mechanical systems have been investigated only in the recent literature. Noteworthy are experiments showing blobs of a liquid composed of micron-size spinning magnets whose surface undulations were attenuated by a shear stress-induced odd normal stress (the shear stress is generated by the collective rotation of the particles close to the free surface, cf. (Soni *et al.* 2019)). In three dimensions Khain *et al.* (2022) showed that odd viscous liquids, in the absence of inertia, give rise to unconventional fluid-flow behavior such as the stabilization of a sedimenting cloud of particles due to an odd viscosity-induced azimuthal velocity field generated by the gravitational stretching of the cloud in the axial direction, in agreement with the physical interpretation of Avron *et al.* (1995). In two dimensions such an odd viscosity-induced azimuthal component can be seen in the radial expansion of a bubble (Ganeshan & Abanov 2017). From a microscopic point of view, the mechanisms that may give rise to an odd viscosity coefficient include broken parity, broken time-reversal and microscopic torques. The latter can be traced back to the literature of liquids endowed with rotational degrees of freedom (Dahler & Scriven 1961) which have been employed in the continuum description of magnetic liquids (Rinaldi 2002; Kirkinis 2017). Other odd viscosity-induced phenomena have been succinctly collected in the recent review by Fruchart *et al.* (2023, Fig. 1).

The stabilizing behavior induced by odd viscosity in (Soni *et al.* 2019) as well as in other references that have appeared in the recent literature (see e.g. (Kirkinis & Andreev 2019)), implies that the odd viscous stress may endow its medium with an intrinsic restoring property. Since the odd viscous stress does not dissipate energy, an excitation given to the fluid may establish an oscillation. Such an oscillation may further initiate wave propagation and periodic expansion and contraction in a plane perpendicular to the propagation direction. This type of motion (in a non-odd viscous liquid) is called an inertial wave and is present in the ocean driving its upper mixing (Asselin & Young 2020), constituting half of its energy and being responsible for the majority of its vertical shear. Inertial waves also appear in the celestial sphere (Ogilvie 2013) and in the technology of propulsion (Gao *et al.* 2020). It has also been argued that inertial waves in the earth's interior are associated with a dynamo dipole and with helicity segregation (Davidson 2014; Davidson & Ranjan 2018). Waves in odd viscous liquids have been investigated in a number of occasions. These include gravity waves (Abanov *et al.* 2018) in incompressible liquids, shock waves (Banerjee *et al.* 2017) and topological sound waves propagating along an interface (Souslov *et al.* 2019) in two-dimensional compressible liquids. Among other reasons, the topological waves are interesting because they are reminiscent of zonal

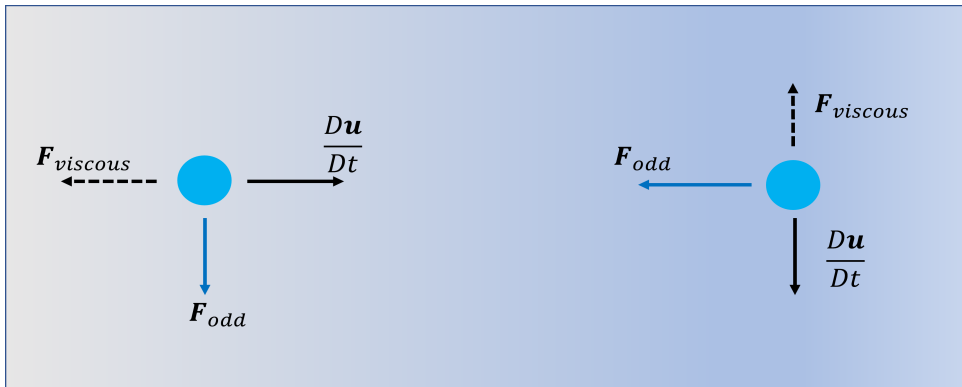


Figure 1: Restoring mechanism associated with odd viscosity in two dimensions. Left: acceleration of a fluid particle is resisted by the viscous force; its odd viscous counterpart acts perpendicularly to the axis of the viscous force. Right: The new tangential motion acquired by the fluid particle is resisted by the viscous force and thus a new odd viscous force acts perpendicularly. The direction of the latter is *opposite* to the original fluid-particle acceleration.

currents associated with wall modes in rapidly-rotating Rayleigh-Bénard convection, although the latter are three-dimensional and are driven by thermal forcing (Knobloch 2022).

A three-dimensional odd viscous liquid may also give rise to Taylor columns. Taylor columns are known to form when bodies move slowly in (non-odd viscous) rapidly rotating liquids (Davidson 2013). For instance, a slowly-moving body along the axis of a rigidly-rotating liquid gives rise to a flow whose component along the axis of rotation can decouple from its lateral plane counterpart (by lateral plane we will mean the plane whose normal is the anisotropy axis). Thus, a Taylor column will form whose speed will be identical to the speed of the slowly-moving body it circumscribes. There are certain restrictive conditions that need to be satisfied in order for a Taylor column to form. These are the small Rossby and Ekman numbers as are defined in Eq. (C1) which thus require high angular velocity of rotation (and slow motions in the rotating frame) and low values of the shear viscosity coefficient. Taylor columns are present in a multitude of diverse areas: cold water and low salinity domes form over seamounts (eg. the Rockall, Faroe and Hutton Banks) of high chlorophyll and nutrient levels enabling larval diversity hotspots (Dransfeld *et al.* 2009) by entrapping plankton (presumably by entraining matter through Stewartson layers). A turbulent ocean below the icy crust of Enceladus and Europa is likely to transfer energy through counter-rotating zonal jets inside a Taylor column (Bire *et al.* 2022).

Taylor columns form in (non-odd viscous) rotating liquids because the Coriolis force is always perpendicular to the velocity field (the latter is expressed in the frame of reference rotating with the liquid). Thus, a radial motion of a fluid particle gives rise to a commensurate azimuthal component and vice-versa. This is reminiscent of the physical interpretation given by Avron *et al.* (1995) to odd viscosity and thus leads to the possibility of observing Taylor columns in such a liquid. As is the case in their rigidly-rotating counterparts, Taylor columns in (non-rotating) odd viscous liquids can be observed when certain restrictions are satisfied. These correspond to the smallness of the parameter $\mathcal{M}^{-1} = \frac{aU}{\nu_0}$ which requires a large coefficient of kinematic odd viscosity ν_o

and slow motions (U can be understood as the velocity of a body moving slowly in an odd viscous liquid) and a is a characteristic length-scale. In addition the effect of shear viscosity ν_e should be small and so should be the Ekman number $\mathcal{J}^{-1} = \frac{\nu_e}{\nu_o}$, see Eq. (6.2).

In Fig. 1 we schematically demonstrate the restoring property induced by odd viscosity on a two-dimensional liquid. In three dimensions, when odd viscosity dominates over its shear counterpart, the restoring behavior can be established *qualitatively* by balancing the inertial terms in the Navier-Stokes equations with the odd viscous term (cf. (Tritton 1988, §16.6) for the case of a rotating liquid). Let $v > 0$ be the velocity of an isolated unit mass fluid particle in a plane perpendicular to the anisotropy axis (say, in the azimuthal direction). Balance between inertia and odd viscous terms leads to

$$\frac{v^2}{r} = \nu_o \frac{v}{r^2} \quad (1.3)$$

giving $v = \frac{\nu_o}{r}$, where $\nu_o = \eta_o/\rho > 0$ is the odd kinematic coefficient of viscosity. Thus, the particle will move in circles of radius $r = \frac{\nu_o}{v}$. The period T_o of this rotation depends on the distance from the axis of anisotropy: $T_o = \frac{2\pi r^2}{\nu_o}$ and this shows that an odd viscous liquid is endowed with an intrinsic frequency

$$\omega_o = \frac{\nu_o}{r^2}. \quad (1.4)$$

Although the above argument is only schematic, the derived expression for the frequency ω_o is recovered in the following quantitative analysis (see Eq. (3.14)), at least in the short wave-length limit. A more satisfying argument supporting the restoring effect of odd viscous liquids is delegated to the end of section 3.1.

In a three dimensional odd viscous liquid we observe waves whose motion resembles the inertial waves occurring in (non-odd viscous) rigidly-rotating liquids. The anisotropy axis inherent in the odd stress plays the role of the rotating axis of a rigidly-rotating liquid. When the inertial-like waves induced by odd viscosity are plane-polarized, there is a superposition of two oppositely directed waves, particle paths are helical and this is reflected in the sign of the helicity density (vorticity times velocity) associated with each direction. When the propagation direction is at right angles to the odd anisotropy axis, the phase velocity vanishes and the system suffers a loss of reflection symmetry (Moffatt 1970). Energy then propagates along the anisotropy axis at maximum group velocity and is accompanied by helicity of a commensurate sign. This effect is called “segregation of helicity” in (non-odd viscous) rigidly-rotating liquids (Davidson & Ranjan 2018) and is believed to be important in understanding the dipolar nature of planetary dynamos since in a planet, mean helicity is spatially segregated having opposite signs at the northern and southern hemispheres, respectively.

In this article we will tacitly assume that such an axis of anisotropy has already been established and proceed by examining the consequences of the resulting odd viscous stress to fluid motions. Here we consider fluid motions in a three-dimensional odd viscous liquid. This paper proceeds in the following manner. In section 2 we describe the constitutive law for the odd viscous liquid that will give rise to the inertial-like waves (Lifshitz & Pitaevskii 1981, §13). Section 3.1 establishes the existence of the inertial-like waves in an odd viscous liquid. These are waves that propagate along the axis of anisotropy and wrapped in coaxial cylinders where liquid does not cross. We theoretically determine the frequency and wavelength of propagated modes. We provide a more satisfying, yet still qualitative discussion of the “elasticity” of an odd viscous liquid. In section 3.4 we numerically solve the full Navier-Stokes equations for the slow motion of a sphere inside

an odd viscous liquid. Such motions generate liquid oscillations downstream the body. Their wavelength is in astonishing agreement to the theoretical value obtained from the inertial theory of section 3.1. In section 3.5 we establish the existence of inertial-like waves exterior to a cylinder and extending to infinity. In section 3.6 we derive the frequency, phase and group velocities of three-dimensional plane-polarized waves. These differ from their axisymmetric counterparts derived in section 3.1 which also vary in the propagation direction. They are also special as they segregate helicity and this is discussed in section 4. In section 5 we derive a modified Taylor-Proudman theorem. This means that when odd viscosity dominates over shear viscosity and inertial terms, the motion in the lateral plane becomes decoupled to the motion of the fluid along the anisotropy axis. This opens up the prospect of existence of Taylor columns in odd viscous liquids, which we explore in section 6. Since the study of Taylor columns entails overwhelming details, in order to provide some structure in our discussion we follow the map set up by Maxworthy (1970) for the slow motion of a particle. We thus solve numerically the Navier-Stokes equations and find many similarities to Maxworthy's work: counterrotating swirling motion above and below the sphere, a forward and a rearward "slug", a stagnant region, indication of an Ekman layer surrounding the sphere etc.

In section 8 we revisit the foregoing results by introducing another part of the odd stress tensor (the η_4 part of the stress in the notation followed by Lifshitz & Pitaevskii (1981, §13 & §58)). This provides a complete picture of odd viscous effects that may be present in a liquid. A consequence of including both viscosity coefficients is the more diverse behavior displayed by the velocity field (it can now resemble Kelvin functions). Helicity is still conserved in such a composite liquid when its velocity field is determined by plane polarized waves. Throughout this paper we compare our results to those of the recent odd viscous liquid literature. Thus, in a dedicated section 9 we summarize the results of these comparisons.

In Appendix A we formulate the odd viscous stress tensor for a three-dimensional liquid in terms of the rate-of-strain tensor, in a manner that is common to the continuum mechanics literature, and thus a compact relation for the full stress incorporating both even (shear) and odd stresses is obtained. This leads directly to the vanishing of the odd stress contribution in viscous heating. Hence, the constitutive law employed in this article represents a non-dissipative liquid. The problems we discuss in this paper present many similarities to flows generated in a rotating liquid and described in a rotating frame of reference. Thus, throughout the paper, where appropriate, we establish connections to these effects. We conclude in Appendix C by outlining a few facts about rotating fluids that are of relevance to this article (although this article is not about rotating liquids).

2. Constitutive relations of a three-dimensional odd viscous liquid

In fluid mechanics the constitutive law (the Cauchy stress tensor) of a *Newtonian* liquid is usually introduced following the phenomenological approach, cf. (Batchelor 1967, §3.3) or more rigorously by employing the principle of objectivity cf. (Truesdell & Noll 1992). It is however possible to also introduce the notion of stress through the Onsager principle of the symmetry of the kinetic coefficients (Lifshitz & Pitaevskii 1981, §13). When these coefficients (here the viscosity tensor $\eta_{\alpha\beta\gamma\delta}$ we introduced in Eq. (1.1)) depend on external fields, say \mathbf{b} , that change sign under time-reversal, the symmetry of the kinetic coefficients is ensured when

$$\eta_{\alpha\beta\gamma\delta}(\mathbf{b}) = \eta_{\gamma\delta\alpha\beta}(-\mathbf{b}). \quad (2.1)$$

For an incompressible liquid the stress tensor (1.1), subject to such a field, obtains the

form

$$\begin{aligned} \sigma'_{\alpha\beta} = & 2V_{\alpha\beta}(\eta + \eta_1) + V_{\beta\gamma} [2(\eta_2 - \eta_1)b_\gamma b_\alpha + \eta_3 b_{\alpha\gamma}] + V_{\alpha\gamma} [2(\eta_2 - \eta_1)b_\gamma b_\beta + \eta_3 b_{\beta\gamma}] \\ & + V_{\gamma\delta} [(\eta_1 + \zeta_1)\delta_{\alpha\beta} b_\gamma b_\delta + (\eta_1 - 4\eta_2)b_\alpha b_\beta b_\gamma b_\delta + (2\eta_4 - \eta_3)(b_{\alpha\gamma} b_\beta b_\delta + b_{\beta\gamma} b_\alpha b_\delta)] \end{aligned} \quad (2.2)$$

where $b_{\alpha\beta} = \epsilon_{\alpha\beta\gamma} b_\gamma$, η_i, ζ_i are viscosity coefficients, $V_{\gamma\delta} = \frac{1}{2} \left(\frac{\partial u_\gamma}{\partial x_\delta} + \frac{\partial u_\delta}{\partial x_\gamma} \right)$ and $\epsilon_{\alpha\beta\gamma}$ is the alternating tensor.

The physical system considered in this paper consists of an odd viscous liquid endowed with odd coefficients η_3 and η_4 in (2.2) and the field \mathbf{b} to lie in the z -direction, so $\mathbf{b} = \dot{\mathbf{z}}$.

The presentation becomes opaque when both coefficients are employed simultaneously. We thus consider each one in turn. Considering only $\eta_3 \neq 0$, we set $\eta = \eta_4 = 0$ and $\eta_2 = \eta_1 = -\zeta_1$. The corresponding odd stress tensor in polar cylindrical coordinates reads (cf. Fig. 2)

$$\boldsymbol{\sigma}' = \eta_o \begin{pmatrix} -(\partial_r v_\phi - \frac{1}{r} v_\phi + \frac{1}{r} \partial_\phi v_r) & \partial_r v_r - \frac{1}{r} v_r - \frac{1}{r} \partial_\phi v_\phi & 0 \\ \partial_r v_r - \frac{1}{r} v_r - \frac{1}{r} \partial_\phi v_\phi & \partial_r v_\phi - \frac{1}{r} v_\phi + \frac{1}{r} \partial_\phi v_r & 0 \\ 0 & 0 & 0 \end{pmatrix}, \quad (2.3)$$

by identifying $\eta_o (> 0)$ with $-\eta_3$. η_o also appears as coefficient $-\eta_1^o$ in (Khain *et al.* 2022). Since the liquid is three-dimensional, there is a third velocity component v_z related to v_r and v_ϕ through the isochoric constraint

$$\partial_r(rv_r) + \partial_\phi v_\phi + r\partial_z v_z = 0. \quad (2.4)$$

For the sake of clarity, in (2.3) we have chosen only one of the coefficients that appear in the stress (2.2) to characterize our odd viscous liquid. This is done so that the fluid flow behavior associated with this coefficient becomes uncoupled to other types. It would be possible to also consider nonzero η_4 (corresponding to η_2^o in (Khain *et al.* 2022)). We thus revisit the current problem in section 8 by considering the η_4 viscosity coefficient in (2.2) both individually and in conjunction to η_o .

In Appendix A we have formulated the odd stress (2.3) in terms of the rate-of-strain tensor in two and in three dimensions which follows more closely the continuum mechanics literature and we employ this formulation to establish the non-dissipative nature of the odd stress.

3. Three-dimensional waves in an odd viscous liquid

3.1. Axisymmetric inertial waves

In this article we tacitly assume the existence of an axis of anisotropy in the z -direction, established by a secondary mechanism such as a magnetic field or rotation, to which, however, we make no reference. Consider an inviscid liquid endowed with odd viscosity as in (2.3) and an axially symmetric wave propagating along the axis of the magnetic field. Following (Landau & Lifshitz 1987, §14), we consider cylindrical polar coordinates r, ϕ, z (cf. Fig. 2), the fields are independent of ϕ , we neglect nonlinear terms (assuming small-amplitude motions) and the time and axial dependence are given by the factor $\exp[i(kz - \omega t)]$ where the frequency ω and wave number k along the axis are both real. Employing the constitutive law (2.3), the linearized equations of motion (see Appendix

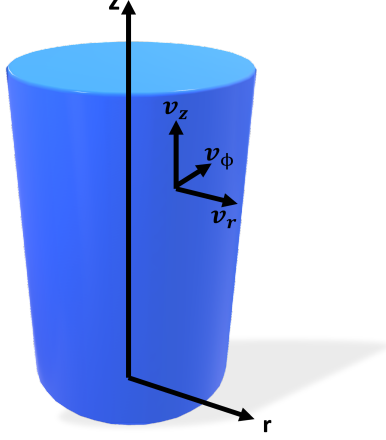


Figure 2: Three-dimensional odd viscous liquid in cylindrical coordinates with velocity field $\mathbf{v} = v_r \hat{\mathbf{r}} + v_\phi \hat{\boldsymbol{\phi}} + v_z \hat{\mathbf{z}}$.

B) become

$$-i\omega v_r = -\frac{1}{\rho} \frac{\partial p'}{\partial r} - \nu_o \left[\frac{1}{r} \frac{\partial}{\partial r} \left(r \frac{\partial v_\phi}{\partial r} \right) - \frac{v_\phi}{r^2} \right], \quad (3.1)$$

$$-i\omega v_\phi = \nu_o \left[\frac{1}{r} \frac{\partial}{\partial r} \left(r \frac{\partial v_r}{\partial r} \right) - \frac{v_r}{r^2} \right], \quad (3.2)$$

$$-i\omega v_z = -\frac{ik}{\rho} p', \quad (3.3)$$

where p' is the variable part of the pressure in the wave and ρ is the liquid's constant density. The equation of continuity is

$$\frac{1}{r} \frac{\partial}{\partial r} (r v_r) + ik v_z = 0. \quad (3.4)$$

Because of Eq. (3.3) and continuity, $p'/\rho = \omega v_z/k = \frac{i\omega}{k^2} \frac{1}{r} \frac{\partial}{\partial r} (r v_r)$ and the identity $\frac{\partial}{\partial r} \left(\frac{1}{r} \frac{\partial}{\partial r} (r v_r) \right) = \frac{1}{r} \frac{\partial}{\partial r} \left(r \frac{\partial v_r}{\partial r} \right) - \frac{v_r}{r^2}$, we obtain $\frac{1}{\rho} \frac{\partial p'}{\partial r} = \frac{i\omega}{k^2} \left[\frac{1}{r} \frac{\partial}{\partial r} \left(r \frac{\partial v_r}{\partial r} \right) - \frac{v_r}{r^2} \right]$. Thus, introducing the linear operator

$$\mathcal{L} = \partial_r^2 + \frac{1}{r} \partial_r - \frac{1}{r^2} \quad (3.5)$$

the r and ϕ momentum equations become

$$-i\omega v_r = -i \frac{\omega}{k^2} \mathcal{L} v_r - \nu_o \mathcal{L} v_\phi, \quad (3.6)$$

$$-i\omega v_\phi = \nu_o \mathcal{L} v_r. \quad (3.7)$$

Expressing the velocities v_r and v_ϕ in terms of Bessel or modified Bessel functions, $v_r = AJ_m(\kappa r)$, $v_\phi = BJ_m(\kappa r)$, or $v_r = AI_m(\kappa r)$, $v_\phi = BI_m(\kappa r)$, etc., (where A and B are constants and κ is an eigenvalue) we find that $m = 1$. With the identity $\mathcal{L} J_1(\kappa r) = -\kappa^2 J_1(\kappa r)$, the system (3.6) and (3.7) has a solution when the determinant $\kappa^4 k^2 \nu_o^2 - \omega^2 (\kappa^2 + k^2)$ of the coefficients of the resulting linear system

$$Ak^2\omega - \kappa^2(i\nu_o Bk^2 - A\omega) = 0, \quad \text{and} \quad i\nu_o A\kappa^2 + \omega B = 0 \quad (3.8)$$

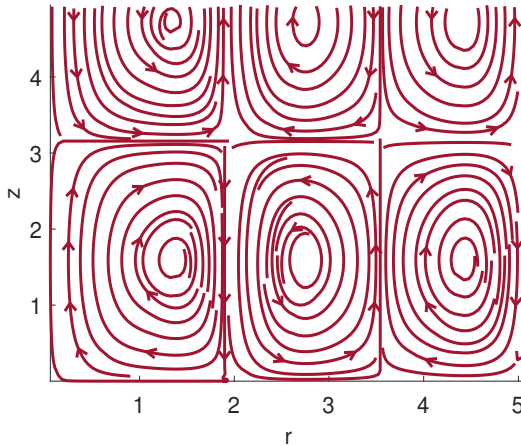


Figure 3: Instantaneous streamlines in the $r - z$ plane with streamfunction (3.15), representing a simple harmonic wave propagating in the z - direction with phase velocity $c_p = \omega/k$ (see Eq. (3.16)). Vertical lines are cross-sections of cylinders wrapping around the central axis and were formed from the zeros of the Bessel function J_1 where $v_r = 0$. The radius b of the external cylinder is determined by the condition $\kappa b = \gamma_3$, where γ_3 is the third root of the Bessel function J_1 in the streamfunction (3.15) or equivalently in the radial velocity field in Eq. (3.10).

vanishes. Consider first the case where the origin is included in the domain. It is not difficult to show that the solution is the Bessel function $J_1(\kappa r)$ for which κ satisfies

$$\kappa^2 = \omega \frac{\omega \pm \sqrt{\omega^2 + (2k^2\nu_o)^2}}{2k^2\nu_o^2}. \quad (3.9)$$

Thus, overall we found

$$v_r = AJ_1(\kappa r)e^{i(kz-\omega t)}, \quad v_\phi = -iA\frac{\nu_o\kappa^2}{\omega}J_1(\kappa r)e^{i(kz-\omega t)}, \quad v_z = iA\frac{\kappa}{k}J_0(\kappa r)e^{i(kz-\omega t)}. \quad (3.10)$$

The motion comprises regions between coaxial cylinders with radius r_n such that

$$r_n\kappa = \gamma_n, \quad (3.11)$$

and γ_n are the zeros of $J_1(x)$. Both v_r and v_ϕ vanish at these coaxial cylinders and the fluid does not cross them. The allowed values of the frequency ω in Eq. (3.9) are not restricted in any way in the infinite medium under consideration (in contrast, in the rotating fluid case where $\kappa = k\sqrt{\frac{4\Omega^2}{\omega^2} - 1}$, the angular velocity Ω of the liquid is required to satisfy the bound $\omega < 2\Omega$, for the solution to be finite). In defining Eq. (3.9) we have tacitly assumed that the solutions we pursue are finite in the radial direction r and have thus discarded κ 's associated with (exponentially increasing/decreasing) modified Bessel function solutions. κ 's in our discussion are always real (this can be justified by choosing large ω for instance).

Employing the radial and azimuthal momentum equations (3.1) and (3.2) we can now give a more satisfying explanation of the “elasticity” of an odd viscous liquid and its tendency to restore a fluid particle back to its original position. Following (Davidson 2013, §1.1) and (Yih 1988, §5), consider a circular ring of fluid in an odd viscous liquid with zero

shear viscosity, wholly located on the x - y plane. By some perturbation, the ring starts moving outwards with velocity $v_r > 0$ and thus expands, so that $\partial_r v_r + \frac{1}{r}v_r + \frac{1}{r}\partial_\phi v_\phi > 0$, where the last expression is the divergence of the velocity field in two dimensions. Rewrite Eq. (3.6)-(3.7) as

$$-i\omega \left(1 + \frac{\kappa^2}{k^2}\right) v_r = F_r, \quad -i\omega v_\phi = F_\phi \quad (3.12)$$

where $F_r \equiv -\nu_o \mathcal{L} v_\phi = \nu_o \kappa^2 v_\phi$ and $F_\phi \equiv \nu_o \mathcal{L} v_r = -\nu_o \kappa^2 v_r$. Since $v_r > 0$ the second of (3.12) implies that there will be an azimuthal force $F_\phi = -\kappa^2 \nu_o v_r < 0$, an acceleration of the liquid in the $-\hat{\phi}$ direction and a commensurate negative velocity v_ϕ , where we employed the eigenvalue $-\kappa^2$ of the linear operator \mathcal{L} in (3.5). This velocity will give rise to a radial force $F_r = -\kappa^2 \nu_o |v_\phi|$ in the first of (3.12). This force endows the ring with an acceleration that points towards the origin, that is, towards the original location of the fluid ring, so it tries to reverse its expansion (the pressure contributes the $-i\omega \frac{\kappa^2}{k^2}$ in (3.12)). As the ring passes through its original position due to inertia and contracts $\partial_r v_r + \frac{1}{r}v_r + \frac{1}{r}\partial_\phi v_\phi < 0$, there will be a new azimuthal velocity component with opposite sign to the above one, that will lead to an eventual expansion towards equilibrium.

3.2. Axial inertial waves interior to a cylinder

We consider the liquid confined within a solid cylindrical surface located, say, at $r = a$, that would be realistic in a laboratory setting. This boundary will be a streamline located at an integral number of cells in the radial direction. If by γ_n we denote the n -th zero of the Bessel function J_1 , Eq. (3.9) with the condition $\kappa a = \gamma_n$ lead to the constraint

$$a \left(\omega - \frac{\omega + \sqrt{\omega^2 + (2k^2\nu_o)^2}}{2k^2\nu_o^2} \right)^{1/2} = \gamma_n, \quad (3.13)$$

and n denotes the number of cells in the radial direction (cf. Fig. 3). From Eq. (3.13) we derive the dispersion relation

$$\omega = \frac{\nu_o k \gamma_n^2}{a \sqrt{k^2 a^2 + \gamma_n^2}}, \quad (3.14)$$

where n denotes the number of cells in the radial direction (for clarity we have suppressed the symbol \pm in (3.14) and only consider the positive sign). It is clear that in the limit $ka \gg \gamma_n$, the frequency in Eq. (3.14) becomes $\omega \sim \frac{\nu_o}{a^2}$ which recovers the qualitative frequency (1.4) we obtained at the Introduction of this article.

In Fig. 3 we plot the streamlines interior to a cylinder of radius b with the instantaneous streamfunction

$$\psi(r, z) = \frac{\kappa}{3.83} r J_1(\kappa r) \sin(kz), \quad v_z = \frac{1}{r} \frac{\partial \psi}{\partial r}, \quad v_r = -\frac{1}{r} \frac{\partial \psi}{\partial z}, \quad (3.15)$$

for $k = 1$ and $\kappa = 2$ for comparison with Fig. 7.6.4 of (Batchelor 1967, p.561) who is employing the same form for the streamfunction with the first zero 3.83 of the Bessel function to modulate the amplitude in the denominator of (3.15). The horizontal lines are locations where $v_r = 0$ (zeros of the Bessel function).

There is important information to be surmised from the phase and group velocities

$$c_p = \frac{\nu_o \gamma_n^2}{a \sqrt{k^2 a^2 + \gamma_n^2}}, \quad \text{and} \quad c_g = \frac{\nu_o \gamma_n^4}{a (k^2 a^2 + \gamma_n^2)^{3/2}}, \quad (3.16)$$

we derive from Eq. (3.14) (we have suppressed the symbol \pm and employed only the

positive sign in (3.14)). Since

$$c_p = c_g + \frac{a\nu_o k^2 \gamma_n^2}{(k^2 a^2 + \gamma_n^2)^{3/2}} > c_g, \quad (3.17)$$

the energy of a disturbance caused by a slowly-moving body along the axis of the cylinder with a velocity equal to c_p , cannot advance upstream relative to the body. Waves will be formed in the downstream direction. We reach the analogous conclusion if we employ the negative sign in (3.14). This situation is thus similar to the rotating liquid case where the energy cannot propagate upstream and thus waves are formed only downstream, as described in many experiments, e.g. those of (Long 1953). We verify these claims in section 3.4 by combining numerical simulations of the Navier-Stokes equations with the theoretical predictions of the present section. (Note how the expression for ω in Eq. (3.14) contrasts with the inviscid liquid rotating at an angular velocity Ω , where $\omega = 2\Omega k / \sqrt{k^2 + (\frac{\gamma_n}{a})^2}$).

3.3. Allowed wave-numbers

When the number of cells in the radial direction is n , from (3.13) allowed wavenumbers supporting propagation with phase velocity $c_p = \omega/k$ and for which the boundary at $r = a$ is a streamline, satisfy

$$ak = \gamma_n \left(\left(\frac{\nu_o \gamma_n}{ac_p} \right)^2 - 1 \right)^{1/2}. \quad (3.18)$$

Wave propagation is thus possible when

$$\frac{ac_p}{\nu_o} < \gamma_n \quad (3.19)$$

where n denotes the number of cells in the radial direction. Thus, although Eq. (3.9) does not introduce a restriction on frequencies for the propagation of waves, Eq. (3.18) does: Defining a Maxworthy number \mathcal{M}_a based on the phase velocity c_p and cylinder radius a (cf. Eq. (6.2) for the definition of the dimensionless number \mathcal{M})

$$\mathcal{M}_a = \frac{\nu_o}{ac_p}, \quad (3.20)$$

inertial motions with n cylinders (n -th zero of J_1) are possible only when

$$\mathcal{M}_a > \frac{1}{\gamma_n}. \quad (3.21)$$

3.4. Numerical determination of odd viscous inertial oscillations inside a cylinder of radius a

By the inequality (3.17) we argued that, based on the inertial waves construction of sections 3.1 - 3.3, the energy of a disturbance caused by a slowly-moving body along the axis of the cylinder with a velocity equal to c_p , cannot advance upstream relative to the body. Waves will be formed in the downstream direction.

To verify this claim we perform numerical simulations of the full Navier-Stokes equations of a slowly-moving body with velocity $U = 0.05$ cm/sec in a cylinder of base radius $a = 25$ cm filled with an odd viscous liquid of dynamic coefficient $\eta_o = 0.7$ g/(cm sec), shear viscosity $\eta = 0.01$ g/(cm sec) and density $\rho = 1.1$ g/cm³. Figure 4 displays the streamlines in the $r - z$ plane of the liquid downstream the moving body which show

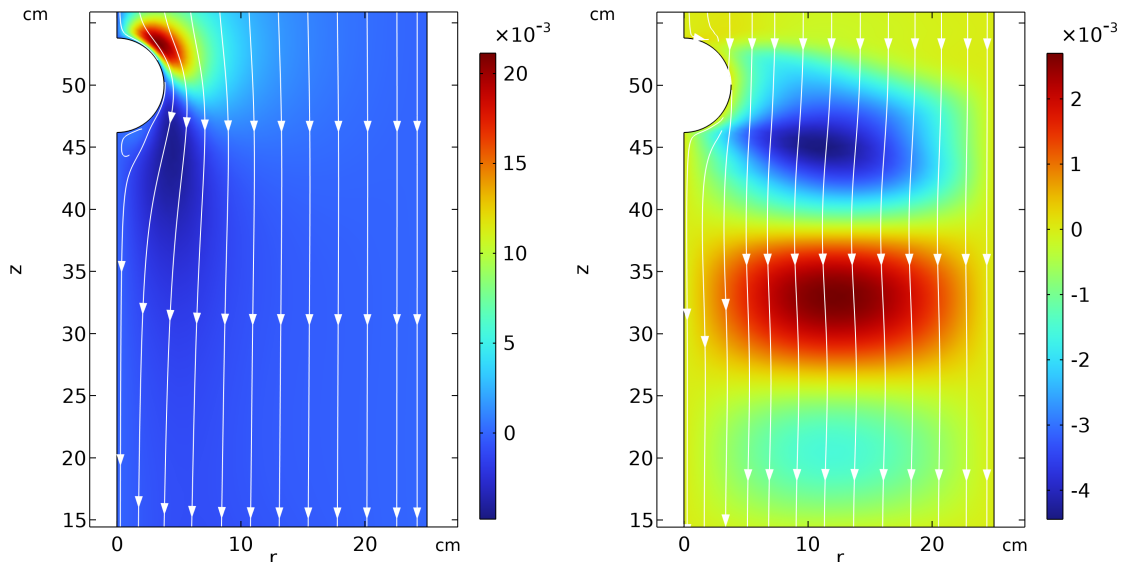


Figure 4: **Right:** Waves generated by a small (3.8 cm) slowly-moving sphere (located at the center of the cylinder - upper left of the figure) in an odd viscous liquid contained in a cylinder of radius 25 cm. The color bar denotes the strength of the radial liquid velocity v_r . Its direction changes sign as we move down and away from the body and it is thus responsible for the distortion of the streamlines (in white). From this plot we can visually determine the wavelength to approximately be 25 cm long. This agrees rather well with the theoretical estimate of 24.476 cm obtained from Eq. (3.22). **Left:** In the absence of odd viscosity no radial disturbance is visible as we move down and away from the body. Colorbar denotes radial velocity. The figure was produced with the finite-element package *comsol* by solving the full Navier-Stokes equations including inertial terms in a three-dimensional axisymmetric domain.

wave-like behavior. To determine the wavelength, the color-bar shows the strength of the radial liquid velocity v_r whose direction changes sign as we move down. From the plot we can visually determine that the wavelength λ is approximately 25 cm long. We compare this estimate to the theoretical prediction of sections 3.1 - 3.3: From Eq. (3.18) we find that

$$\lambda = \frac{2\pi}{k} = \frac{2\pi a}{\gamma_1 \sqrt{\left(\frac{\nu_o \gamma_1}{aU}\right)^2 - 1}} = 24.4764 \text{ cm} \quad (3.22)$$

where $\gamma_1 = 3.8317$ is the first root of the Bessel function J_1 . Figure 4 was produced with the finite-element package *comsol* by solving the full Navier-Stokes equations in a three-dimensional axisymmetric domain. The flow Reynolds number, based on cylinder radius $a = 25$ cm is 125.

This situation is thus analogous to the rotating liquid case where the energy cannot propagate upstream and thus waves are formed only downstream, as described by the experiments of Long (1953), cf. (Batchelor 1967) pp.564-6 and plate 24.

3.5. Axial inertial waves exterior to a cylinder

The above discussion can also be employed to establish wave propagation when the odd viscous liquid occupies the region $r > a$, exterior to a solid cylinder located at $r = a$.

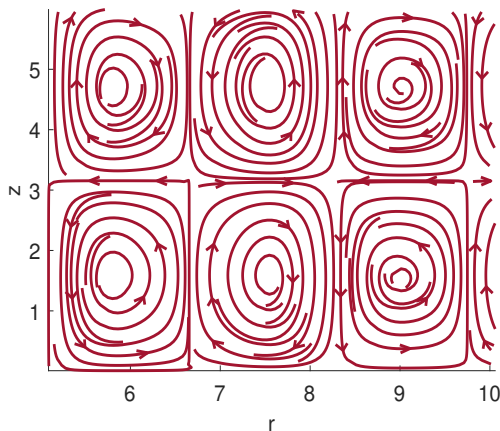


Figure 5: Instantaneous streamlines exterior to a cylinder of radius $r = \frac{\alpha_3}{\kappa}$ where α_3 is the third zero of Y_1 . This is simple harmonic wave propagating in the z - direction with phase velocity ω/k . Vertical lines correspond to zeros of the Bessel function of second kind Y_1 where $v_r = 0$.

Now, the solution is of the form of a Bessel function of the second kind in the radial coordinate

$$v_r = AY_1(\kappa r)e^{i(kz-\omega t)}, \quad v_\phi = -iA\frac{\nu_o\kappa^2}{\omega}Y_1(\kappa r)e^{i(kz-\omega t)}, \quad v_z = iA\frac{\kappa}{k}Y_0(\kappa r)e^{i(kz-\omega t)} \quad (3.23)$$

and the results of the previous sections hold with the replacement

$$J_1 \rightarrow Y_1, \quad \gamma_n \rightarrow \alpha_n, \quad (3.24)$$

where α_n is the n th zero of $Y_1(x)$. In Fig. 5 we plot the streamlines exterior to a cylinder of radius b with the instantaneous streamfunction

$$\psi(r, z) = \frac{\kappa}{3.83}rY_1(\kappa r)\sin(kz), \quad v_z = \frac{1}{r}\frac{\partial\psi}{\partial r}, \quad v_r = -\frac{1}{r}\frac{\partial\psi}{\partial z} \quad (3.25)$$

for $k = 1$ and $\kappa = 2$ for comparison with Fig. 7.6.4 of (Batchelor 1967, p.561).

3.6. Plane-polarized waves induced by odd viscosity

The axisymmetric inertial waves we discussed earlier propagate along the z - axis (the axis of anisotropy) and are three-dimensional in the sense that the wave amplitude varies along both the propagation direction and normal to it. In this section we will consider different types of inertial waves that propagate along an arbitrary direction and are polarized in the plane perpendicular to the propagation axis. This section follows the notation of (Landau & Lifshitz 1987, §14). The odd-viscous Navier-Stokes equations

$$\frac{D\mathbf{v}}{Dt} = -\frac{1}{\rho}\nabla p + \nu_o\nabla_2^2\hat{\mathbf{z}} \times \mathbf{v}, \quad (3.26)$$

where $\nabla_2^2 = \partial_x^2 + \partial_y^2$ and D/Dt is the convective derivative, become after taking the curl of both sides

$$\frac{D}{Dt}\text{curl}\mathbf{v} = \text{curl}\mathbf{v} \cdot \nabla\mathbf{v} - \nu_o\nabla_2^2\frac{\partial\mathbf{v}}{\partial z}. \quad (3.27)$$

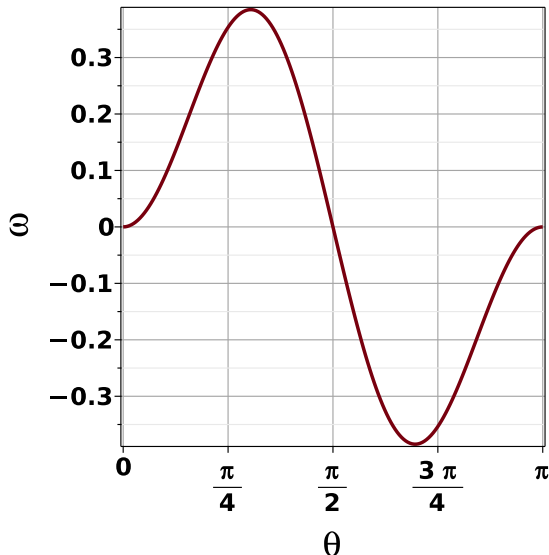


Figure 6: Section 3.6 plane-polarized wave dispersion ω (Eq. (3.32)) versus angle θ between the wavevector \mathbf{k} and the z - (anisotropy) axis (setting $k = \nu_o = 1$). Of interest is the low frequency range at $\theta \sim \frac{\pi}{2}$ where group velocity is maximum. This curve structure should be contrasted to the corresponding relation $\omega = 2\Omega \cos \theta$ of an inviscid fluid rotating with angular velocity Ω .

Linearizing,

$$\partial_t \text{curl} \mathbf{v} = -\nu_o \nabla^2 \frac{\partial \mathbf{v}}{\partial z}, \quad (3.28)$$

we seek plane-wave solutions of the form

$$\mathbf{v} = \mathbf{A} e^{i(\mathbf{k} \cdot \mathbf{r} - \omega t)}, \quad (3.29)$$

where \mathbf{A} is normal to \mathbf{k} from the incompressibility condition.

Substituting the plane-wave solution into (3.28) we obtain

$$\omega \mathbf{k} \times \mathbf{v} = i\nu_o (k_x^2 + k_y^2) k_z \mathbf{v}. \quad (3.30)$$

Taking the cross product of both sides of Eq. (3.30) with \mathbf{k} we obtain

$$-\omega k^2 \mathbf{v} = i\nu_o (k_x^2 + k_y^2) k_z \mathbf{k} \times \mathbf{v}. \quad (3.31)$$

System (3.30)-(3.31) has a solution when the determinant of the coefficients vanishes. Solving for ω we obtain

$$\omega = \pm \frac{\nu_o (k_x^2 + k_y^2) k_z}{k}, \quad \text{or} \quad \omega = \pm \nu_o k^2 \cos \theta \sin^2 \theta, \quad (3.32)$$

where $k = \sqrt{k_x^2 + k_y^2 + k_z^2}$ and the latter equation implies that θ is the angle between the \mathbf{k} and the anisotropy axis. In Fig. 6 we plot the dispersion ω (Eq. (3.32)) versus angle θ between the wavevector \mathbf{k} and the z - (anisotropy) axis. It differs qualitatively from the corresponding relation

$$\omega = 2\Omega \cos \theta \quad (3.33)$$

of a (non-odd viscous) inviscid fluid rotating with angular velocity Ω , cf. (Greenspan

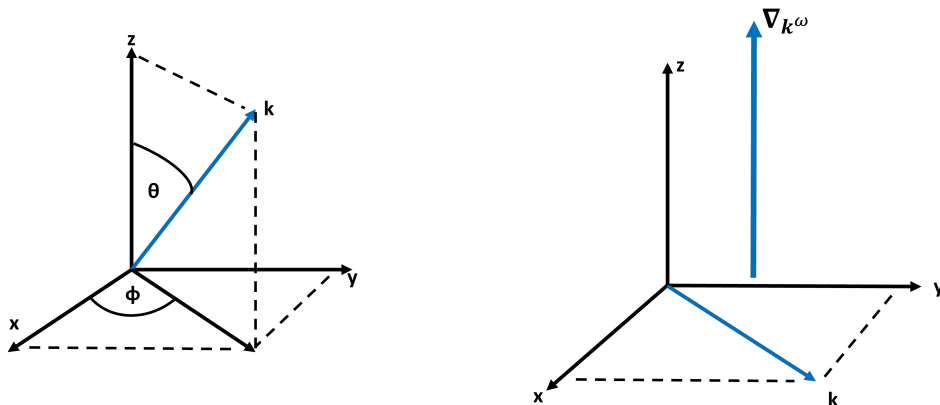


Figure 7: **Left:** coordinate system employed in plane-polarized waves showing the definition of angles for the propagation wavevector \mathbf{k} . **Right:** When the propagation direction is normal to the axis $\hat{\mathbf{z}}$, the group velocity $\mathbf{c}_g = \nabla_{\mathbf{k}}\omega$ in (3.38) becomes co-axial to the axis $\hat{\mathbf{z}}$ and acquires its maximum value.

1968). Comparing Eq. (3.32) with (3.33), when the coefficients ν_o and Ω are kept constant, it becomes evident that the dispersion relation (3.32) obtained due to the specific form of the constitutive law (2.3) we adopted for an odd viscous liquid becomes prominent for large in-plane wave numbers and small corresponding wavelengths.

Following Landau & Lifshitz (1987), we introduce the unit vector $\hat{\mathbf{k}} = \frac{\mathbf{k}}{k}$ in the direction of the wave-vector and the complex amplitude $\mathbf{A} = \mathbf{a} + i\mathbf{b}$ where \mathbf{a} and \mathbf{b} are real vectors. Considering Eq. (3.30) and the dispersion relation (3.32) we obtain $\hat{\mathbf{k}} \times \mathbf{b} = \mathbf{a}$, that is, the two vectors \mathbf{a} and \mathbf{b} are perpendicular to each other, are of the same magnitude and lie in the plane whose normal is \mathbf{k} . Thus, the velocity field is circularly polarized in the plane defined by \mathbf{a} and \mathbf{b} and is of the form

$$\mathbf{v} = \mathbf{a} \cos(\mathbf{k} \cdot \mathbf{r} - \omega t) - \mathbf{b} \sin(\mathbf{k} \cdot \mathbf{r} - \omega t), \quad \mathbf{a} \perp \mathbf{b}. \quad (3.34)$$

Employing the negative sign of the dispersion relation (3.32), the above analysis leads to the same velocity field (3.34) but with the sense of the vectors \mathbf{a} and \mathbf{b} reversed: $\hat{\mathbf{k}} \times \mathbf{b} = -\mathbf{a}$. This will become important in section 4 where the helicity associated with wave propagation will be determined.

It is of interest to calculate the direction of propagation of energy. We obtain

$$\frac{\partial \omega}{\partial k_x} = \nu_o \frac{k_x k_z (k^2 + k_z^2)}{k^3}, \quad \frac{\partial \omega}{\partial k_y} = \nu_o \frac{k_y k_z (k^2 + k_z^2)}{k^3}, \quad \frac{\partial \omega}{\partial k_z} = \nu_o \frac{(k_x^2 + k_y^2)^2}{k^3} \quad (3.35)$$

or, taking the z axis to be the axis of anisotropy we obtain

$$\left(\frac{\partial \omega}{\partial k_x}, \frac{\partial \omega}{\partial k_y} \right) = k \nu_o \sin \theta \cos \theta (1 + \cos^2 \theta) (\cos \phi, \sin \phi), \quad \frac{\partial \omega}{\partial k_z} = k \nu_o \sin^4 \theta. \quad (3.36)$$

The group velocity $\mathbf{c}_g = \frac{\partial \omega}{\partial \mathbf{k}}$ in vector form can be written as

$$\frac{\partial \omega}{\partial \mathbf{k}} = \nu_o k \left\{ \hat{\mathbf{k}} (\hat{\mathbf{z}} \cdot \hat{\mathbf{k}}) \left[1 + (\hat{\mathbf{z}} \cdot \hat{\mathbf{k}})^2 \right] + \hat{\mathbf{z}} \left[1 - 3(\hat{\mathbf{z}} \cdot \hat{\mathbf{k}})^2 \right] \right\}, \quad (3.37)$$

which can be compared with its rigidly-rotating (non-odd viscous) counterpart $\frac{\partial \omega}{\partial \mathbf{k}} = \frac{2\Omega}{k} \left[\hat{\mathbf{z}} - \hat{\mathbf{k}} (\hat{\mathbf{z}} \cdot \hat{\mathbf{k}}) \right]$ where the group velocity is perpendicular to the phase velocity $\mathbf{c}_p = \frac{\omega}{k} \hat{\mathbf{k}}$

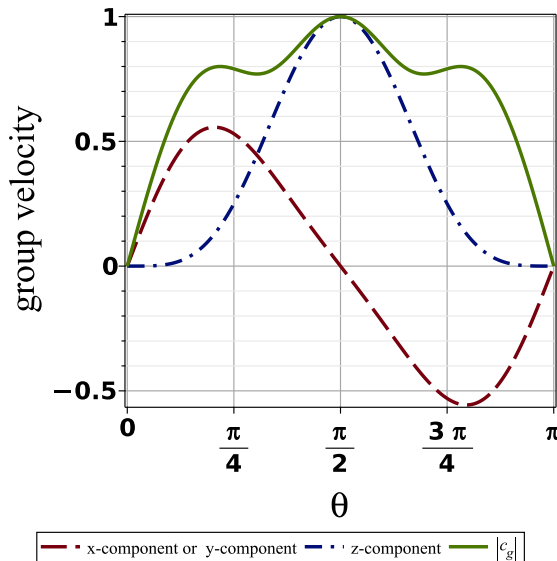


Figure 8: Section 3.6 plane-polarized wave group velocity components and magnitude Eq. (3.36) and (3.38) versus angle θ between the wavevector \mathbf{k} and the z - (anisotropy) axis, setting $k = \nu_o = 1$ (and $\phi = \pi/4$, for simplicity). Of interest is the low frequency range at $\theta \sim \frac{\pi}{2}$ where group velocity is maximum. The modulus of the group velocity should be contrasted to $|\frac{\partial\omega}{\partial\mathbf{k}}| = (2\Omega/k) \sin\theta$ in the case of an inviscid rigidly rotating liquid with angular velocity Ω .

(see Table 1). Here the group velocity is not perpendicular to the phase velocity. A calculation gives $\mathbf{c}_g \cdot \mathbf{c}_p = 2|\mathbf{c}_p|^2 = 2\nu_o^2 k^2 \cos^2\theta \sin^4\theta$. Thus, in contrast to the case of inertial waves in a rotating fluid where the energy propagates perpendicularly to the wave-vector, here the energy propagation direction has a component along the $\hat{\mathbf{k}}$ axis. The modulus of the group velocity is

$$\left| \frac{\partial\omega}{\partial\mathbf{k}} \right| = k\nu_o \sin\theta \sqrt{5 \cos^4\theta - 2 \cos^2\theta + 1}. \quad (3.38)$$

In Fig. 8 we plot the group velocity components Eq. (3.36) and its magnitude (3.38) versus angle θ between the wavevector \mathbf{k} and the z - (anisotropy) axis (setting $k = \nu_o = 1$).

In addition to the information of Table 1, the frequency is maximum at $\theta = \cos^{-1} \frac{\sqrt{3}}{3} \sim 0.3\pi$, it acquires the value $\omega = \pm\nu_o k^2 \frac{2\sqrt{3}}{9}$. The group velocity becomes $\frac{4k\nu_o}{9}(\sqrt{2} \cos\phi, \sqrt{2} \sin\phi, 1)$ and its modulus is $c_g = 4k\nu_o\sqrt{3}/9$. In addition the group velocity has a local maximum at $\theta = \cos^{-1} \frac{\sqrt{15}}{5} \sim 0.22\pi$. The frequency is $\omega = \pm\nu_o k^2 \frac{2\sqrt{15}}{25}$ and the group velocity becomes $\frac{4k\nu_o}{25}(2\sqrt{6} \cos\phi, 2\sqrt{6} \sin\phi, 1)$ and its modulus is $c_g = 4k\nu_o/5$. Comparison can be made of Eq. (3.38) with plane-polarized waves rigidly rotating (Landau & Lifshitz 1987, §14) where $|\frac{\partial\omega}{\partial\mathbf{k}}| = (2\Omega/k) \sin\theta$.

4. Conservation of helicity of inertial waves in an odd viscous liquid

Helicity \mathcal{H} ,

$$\mathcal{H} = \int_V \mathbf{v} \cdot \text{curl}\mathbf{v} dV = \text{constant}, \quad (4.1)$$

	odd viscous liquid	rigidly-rotating liquid
low ω :	$\mathbf{k} \parallel \boldsymbol{\Omega}$; $c_g = 0$ and $\mathbf{k} \perp \boldsymbol{\Omega}$; $\mathbf{c}_g = \pm \nu_o k \hat{\mathbf{z}}$ (max)	$\mathbf{k} \perp \boldsymbol{\Omega}$; $\mathbf{c}_g = \frac{\pm 2\Omega \hat{\mathbf{z}}}{k}$ (max)
high ω :	$\theta = \cos^{-1} \frac{\sqrt{3}}{3} \sim 0.3\pi$	$\mathbf{k} \parallel \boldsymbol{\Omega}$; $\mathbf{c}_g = 0$
$\mathbf{c}_p \cdot \mathbf{c}_g$	$2 \mathbf{c}_p ^2$	0
$\mathbf{v} \cdot \text{curl} \mathbf{v}$	$\mp k \mathbf{v} ^2$	$\mp k \mathbf{v} ^2$

Table 1: Summary of odd viscous plane-polarized inertial waves behavior at low and high frequencies (3.32) and comparison with their rigidly-rotating counterparts. \mathbf{c}_g is the group velocity $\frac{\partial \omega}{\partial \mathbf{k}}$ and $\mathbf{c}_p = \frac{\omega}{k} \hat{\mathbf{k}}$ is the phase velocity. The group velocity is maximum when the angle $\theta = \pi/2$, propagation takes place perpendicular to the anisotropy axis ($\hat{\mathbf{z}}$), the group velocity acquires its maximum propagating along the anisotropy axis and helicity becomes segregated, cf. section 4. Helicity density $\mathbf{v} \cdot \text{curl} \mathbf{v}$ has the same functional form in both odd viscous and rigidly-rotating liquids. Although in a rigidly rotating liquid the group velocity is always perpendicular to the phase velocity, in an odd viscous liquid there is dependence on the angle θ (see the third line of the Table). θ denotes the angle between $\boldsymbol{\Omega} = \Omega \hat{\mathbf{z}}$ and the propagation direction \mathbf{k} , cf. Fig. 7.

was shown by Moffatt (1969) to be an invariant of inviscid fluid motion when $\hat{\mathbf{n}} \cdot \text{curl} \mathbf{v}$ vanishes on any closed orientable surface moving with the liquid. Here, we show that, analogously to the rigidly-rotating case, the vorticity of an odd viscous liquid is proportional to the velocity field. For plane-polarized inertial waves this implies that helicity is conserved. Since a number of effects appearing in the literature, such as the emission of inertial waves in a turbulent flow (Davidson 2013, Fig. 3.3(b)) are related to helicity and its sign, we include some discussion below on the presence of helicity in odd viscosity-induced inertial waves.

4.1. Conservation of helicity in plane-polarized waves of an odd viscous liquid

From the plane-polarized velocity field (3.34) we obtain $\text{curl} \mathbf{v} = -\mathbf{k} \times \mathbf{b} \cos(\mathbf{k} \cdot \mathbf{r} - \omega t) - \mathbf{k} \times \mathbf{a} \sin(\mathbf{k} \cdot \mathbf{r} - \omega t)$. The relation $\hat{\mathbf{k}} \times \mathbf{b} = \pm \mathbf{a}$ (the \pm symbol corresponds to the sign of the dispersion relation (3.32)) leads to $\text{curl} \mathbf{v} = \mp k \mathbf{v}$ and thus

$$\mathbf{v} \cdot \text{curl} \mathbf{v} = \mp k |\mathbf{v}|^2 \quad \text{and} \quad \mathcal{H} = \int_V \mathbf{v} \cdot \text{curl} \mathbf{v} dV = \mp k |\mathbf{v}|^2 V, \quad (4.2)$$

where $|\mathbf{v}|^2 = |\mathbf{a}|^2 + |\mathbf{b}|^2$ is the constant magnitude of the velocity in Eq. (3.34), V is the volume of the region under consideration and $k = \sqrt{k_x^2 + k_y^2 + k_z^2}$. The negative sign in (4.2) (corresponding to the positive sign in the dispersion relation (3.32)) is associated with particle paths following left-handed helices and the positive sign with right-handed helices. Energy propagates along a cone whose normal is the vector $\hat{\mathbf{k}}$, (cf. (Davidson 2013) for the case of rigidly rotating liquid).

Inertial-like waves give rise to maximal helicity. This can be seen by substituting Eq. (4.2) into the the Cauchy-Schwartz inequality $\mathcal{H}^2 \leq \mathcal{E} \mathcal{W}$ expressed in terms of the helicity (4.1) and the energy and enstrophy integrals (Moffatt 1969)

$$\mathcal{E} = \int_V \mathbf{v}^2 dV, \quad \mathcal{W} = \int_V \text{curl} \mathbf{v}^2 dV. \quad (4.3)$$

As shown by Moffatt (1970) for the case of rigidly-rotating liquids, inertial waves

exhibit a loss of reflection symmetry when the energy propagates parallel to the rotation axis (and the phase velocity is perpendicular to this axis). Davidson (2013) associates each direction of propagation of energy with one of the signs of helicity in (4.2). Negative sign of helicity for energy propagating in the $+\hat{z}$ direction and positive sign of helicity for energy propagating in the $-\hat{z}$. This is called the “segregation of helicity” and has found applications in problems of magnetohydrodynamics (Davidson 2013; Davidson & Ranjan 2018). The waves that correspond to this type of behavior have low frequencies (the frequency ω in Eq. (3.32) is nearly zero). The consequence of this behavior in an odd viscous liquid can more easily be seen by going back to the original equation of motion (3.26). Linearizing, and taking the limit $\omega \rightarrow 0$ amounts to dropping the time derivative. Then, the equation of motion becomes (5.1) of the foregoing section, that makes the dynamics effectively two-dimensional (perpendicular to the anisotropy axis), leads to the Taylor-Proudman theorem and gives rise to Taylor columns.

4.2. Helicity in axisymmetric inertial waves of an odd viscous liquid

It turns out that vorticity is also parallel to the velocity field for the inertial waves of section 3.1. This can be shown directly by taking the curl of the velocity field (3.10) and solving in expression (3.9) for the frequency, $\omega = \frac{\nu_o k \kappa^2}{\sqrt{k^2 + \kappa^2}}$ (in contrast to the previous section, k here denotes the wave number k_z along the axis, cf. section 3.1). Alternatively, setting $A = ae^{i\theta}$ for real amplitude a and phase θ we obtain

$$v_r = aJ_1(\kappa r) \cos(kz - \omega t + \theta), \quad v_\phi = \frac{\nu_o \kappa^2}{\omega} aJ_1(\kappa r) \sin(kz - \omega t + \theta), \quad (4.4)$$

and $v_z = -\frac{\kappa}{k} aJ_0(\kappa r) \sin(kz - \omega t + \theta)$. In either case the final result is

$$\text{curl} \mathbf{v} = \mp \sqrt{k^2 + \kappa^2} \mathbf{v}, \quad \text{and} \quad \mathbf{v} \cdot \text{curl} \mathbf{v} = \mp \sqrt{k^2 + \kappa^2} |\mathbf{v}|^2. \quad (4.5)$$

When the liquid is contained in a solid cylinder of radius b , ω is replaced by Eq. (3.14) and κ by γ_n/b , where γ_n is the n -th zero of $J_1(x)$.

5. Modified Taylor-Proudman Theorem

For simplicity we consider Cartesian coordinates. The “geostrophic” form (i.e. Navier-Stokes with odd viscosity, without inertia and without shear viscosity) of the equations is

$$\frac{1}{\rho} \frac{\partial p}{\partial x} = -\nu_o \nabla_2^2 v, \quad \frac{1}{\rho} \frac{\partial p}{\partial y} = \nu_o \nabla_2^2 u, \quad \frac{\partial p}{\partial z} = 0, \quad (5.1)$$

where $\nabla_2^2 = \partial_x^2 + \partial_y^2$. This reduction is possible by invoking the requirement $u \ll \nu_o/\ell$ where u and ℓ are characteristic velocity and length scales respectively. This inequality can be derived by balancing the inertial terms $\mathbf{v} \cdot \nabla \mathbf{v} \sim u^2/\ell$ with the odd viscous term $\nu_o \nabla_2^2 u \sim \nu_o u/\ell^2$ and requiring that latter is dominant.

Differentiating the first two with respect to z and considering the third we obtain

$$\nabla_2^2 \partial_z u = 0, \quad \text{and} \quad \nabla_2^2 \partial_z v = 0. \quad (5.2)$$

Eliminating the pressure by cross differentiation of the first two equations we obtain

$$\nabla_2^2 (\partial_x u + \partial_y v) = 0. \quad (5.3)$$

Thus, from continuity we also obtain

$$\nabla_2^2 \partial_z w = 0. \quad (5.4)$$

Defining

$$(U, V, W) = \ell^2 \nabla_2^2 (u, v, w), \quad (5.5)$$

(the length-scale is determined, for instance from the size of the vessel) we derive the Taylor-Proudman theorem for the velocity field U, V, W , that is

$$\partial_z U = \partial_z V = \partial_z W = 0 \quad (5.6)$$

and this can be considered as a liquid in a frame rotating with angular velocity $\Omega = \nu_o \ell^{-2}$. Thus, when the odd viscosity terms are larger than inertia, there is a superposition of a two-dimensional motion in the lateral ($x - y$) plane and a vertical motion, independent of z .

Some familiar behavior at a boundary can also be recovered. Because of the no-penetration condition $w = 0$ on a solid boundary we have $W = 0$ on the same boundary ($(\partial_x^2 + \partial_y^2)w$ must be zero on the boundary). Thus, when a streamline parallel to the axis meets a stationary boundary, this implies that W is zero everywhere.

For axisymmetric systems a further simplification takes place. letting $V_r = \mathcal{L}v_r$ and $V_\phi = \mathcal{L}v_\phi$ where \mathcal{L} was defined in Eq. (3.5), equations (5.1) become

$$\nu_o V_\phi = -\frac{1}{\rho} \frac{\partial p}{\partial r} \quad \text{and} \quad -\nu_o V_r = 0. \quad (5.7)$$

Thus, V_r is zero everywhere and the flow proceeds in spirals. With $V_z = \mathcal{L}v_z$ the continuity equation becomes $\partial_r V_r + \partial_z V_z = 0$. Thus, $\partial_z V_z = 0$ everywhere, giving rise to the Taylor-Proudman theorem.

6. Taylor columns in an odd viscous liquid

The Navier-Stokes equations (5.1) written in the form

$$\frac{1}{\rho} \frac{\partial p}{\partial x} = -\frac{\nu_o}{L^2} V, \quad \frac{1}{\rho} \frac{\partial p}{\partial y} = \frac{\nu_o}{L^2} U, \quad \frac{\partial p}{\partial z} = 0, \quad (6.1)$$

by employing the definition of U, V and W in Eq. (5.5), are suggestive of the existence of Taylor columns in an odd viscous liquid. By this we mean that when an axisymmetric body moves slowly in an odd viscous liquid, a column or a “slug” will be pushed ahead of the body with zero axial velocity relative to the body. In the inviscid limit implied by Eq.(6.1) (meaning the shear viscosity is zero), the column is a cylinder but it will be modified by the presence of shear viscosity. A rear slug will also be present. In general the motion of the liquid in the slug can not be determined from the simple equations (6.1). In reality a number of boundary layers exist which act as a conduit that transports liquid between different locations.

The determination of the flow structure is not only difficult but also changes dramatically when one alters the parameters and the geometry. Taylor columns were studied in the past in the context of slowly moving bodies immersed in a liquid rotating rigidly, see for instance the following comprehensive references (Moore & Saffman 1968; Maxworthy 1970; Tanzosh & Stone 1994; Bush *et al.* 1994) and references therein.

We can define some useful dimensionless parameters for the odd viscosity dominated problems, such as the Taylor \mathcal{T} and Maxworthy \mathcal{M} numbers (Maxworthy (1970) employed the notation N to denote the rotating counterpart of the latter)

$$\mathcal{T} = \frac{\nu_o}{\nu_e}, \quad \mathcal{M} = \frac{\nu_o}{aU}. \quad (6.2)$$

The Taylor number can be understood as an inverse Ekman number denoting the strength

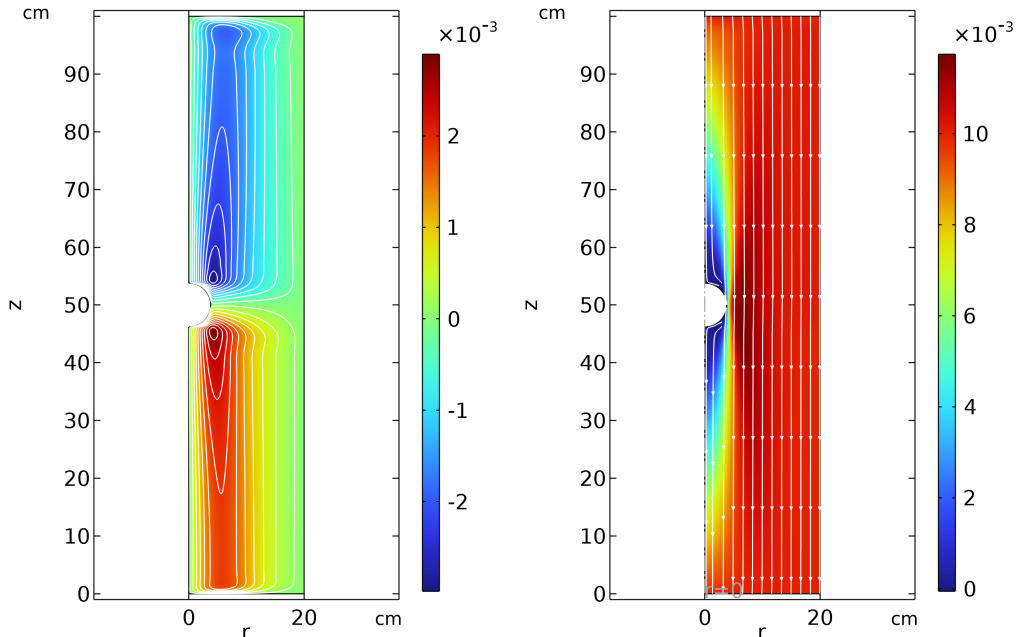


Figure 9: Distribution of azimuthal (left panel) and axial velocity (right panel) in an odd liquid moving slowly and meeting an immobile sphere (of radius 3.8 cm) located at elevation $z = 50$ cm at the center axis of a cylinder. Liquid enters from the top ($z = 100$ cm) and exits at the bottom ($z = 0$). The sphere is not allowed to rotate. Counter-rotation of liquid takes place above and below the sphere in the azimuthal direction (this was also observed by Khain *et al.* (2022, Fig.4(c)) for the analogous problem in Stokes flow). A Taylor-type column is also visible in the right panel, symmetrically placed above and below the sphere

of odd to even viscosity (angular velocity to even viscosity in the rotating fluid case) and the Maxworthy number is the ratio of odd viscous force to inertial forces or the odd viscosity-induced inertial wave propagation velocity to convection velocity.

We can compare the Maxworthy number \mathcal{M} in (6.2) for an odd viscous liquid to the inverse Rossby number $\text{Ro}^{-1} = \frac{\Omega a}{U}$ in (C1) when the parameters ν_o and Ω are held constant. It is clear that Taylor columns in an odd viscous liquid are favored at small (in-plane) length scales, while Taylor columns are favored at large length-scales in rigidly-rotating liquids. This is clear due to the fact that odd viscosity multiplies second order spatial derivatives. Even if its value is small and unimportant in general, observable effects will be present close to boundaries, such as sharp boundary-layers. Thus, one should consider odd viscous effects (described by the specific constitutive law (2.3)) under the restrictions posed by this discussion, which might limit the applicability of the odd viscous liquids in comparison to their (non-odd viscous) rotating counterparts.

The pressure p is a streamfunction and thus constant on a streamline of the flow (U, V, W) . A finite-length cylinder with generators parallel to the rotating axis and moving horizontally in a rotating liquid will have a liquid velocity parallel to its generators and a column will accompany its motion (Yih 1988, §12.2). Likewise, a solid body translating slowly along the axis of the cylinder will be accompanied by a column of fluid with generators parallel to the axis.

Figures 9 and 10 display the salient features of Taylor columns in odd viscous liquids.

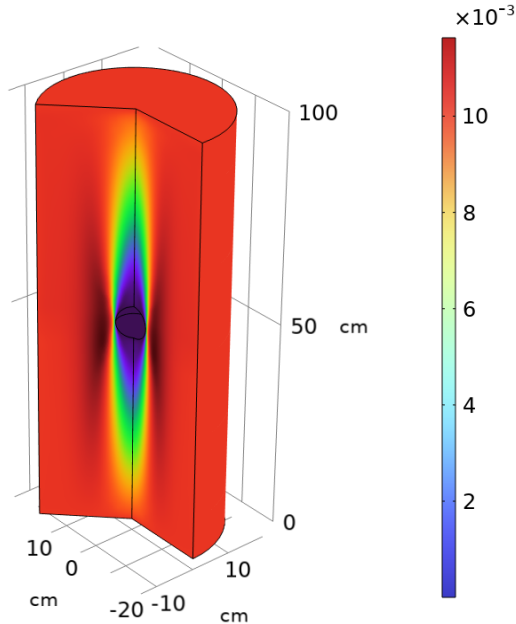


Figure 10: Three-dimensional realization of odd viscous flow around an immobile sphere (of radius 3.8 cm) located at elevation $z = 50$ in a moving cylinder with liquid entering from the top ($z = 100$ cm) and exiting at the bottom ($z = 0$), with the cylinder speed (the sphere is not allowed to rotate). Color-bar denotes the strength of the axial velocity w . A Taylor column of low axial velocity is visible circumscribing the sphere and surrounding the central axis. Parameters employed in to produce this figure: Odd viscosity coefficient $\eta_o = 0.5$ g/(cm sec), shear viscosity $\eta = 0.01$ g/(cm sec), cylinder radius 20 cm, sphere radius 3.8 cm, cylinder height $H = 100$ cm, liquid density $\rho = 1$ g/cm³, liquid velocity in the $-\hat{z}$ direction $U = 0.01$ cm/sec. These give a Taylor number based on the sphere length-scale $\mathcal{T} = 50$ and Maxworthy number $\mathcal{M} = 26.316$, see Eq. (6.2).

Liquid flow entering from the top of a cylinder encounters an immobile sphere located at the central axis. The two “slugs” located above and below the sphere in Figures 9 (right panel) and 10 are characterized by the sharp blue color. There is a swirling flow that takes place above and below the sphere with opposite sense of rotation, Figure 9 (left panel). This is further discussed below.

The exact form of a flow associated with Taylor columns induced by a solid body is a complicated problem depending on parameter regimes (Ekman, Reynolds and Rossby numbers) as well as the geometry (finite or infinite cylinder), geometry of the body and ultimately, its constitution (whether it is a solid or a liquid). Here we will not pause to carry-out a detailed enumeration of special cases arising in the various parameter regimes, geometries and materials; we will only point-out certain qualitative similarities that exist between an odd viscous liquid and rigidly rotating flow.

Figure 11 displays azimuthal and axial velocities of the liquid flowing in the cylinder of Figures 9 and 10. Probes located at different elevations of the cylinder measure velocities as they vary in radial direction, from the cylinder central axis to its external surface, with a view to compare our results to the experiments of Maxworthy (1970). In these numerical simulations the Taylor and Maxworthy numbers are $\mathcal{T} = 50$ and $\mathcal{M} = 26$, respectively.

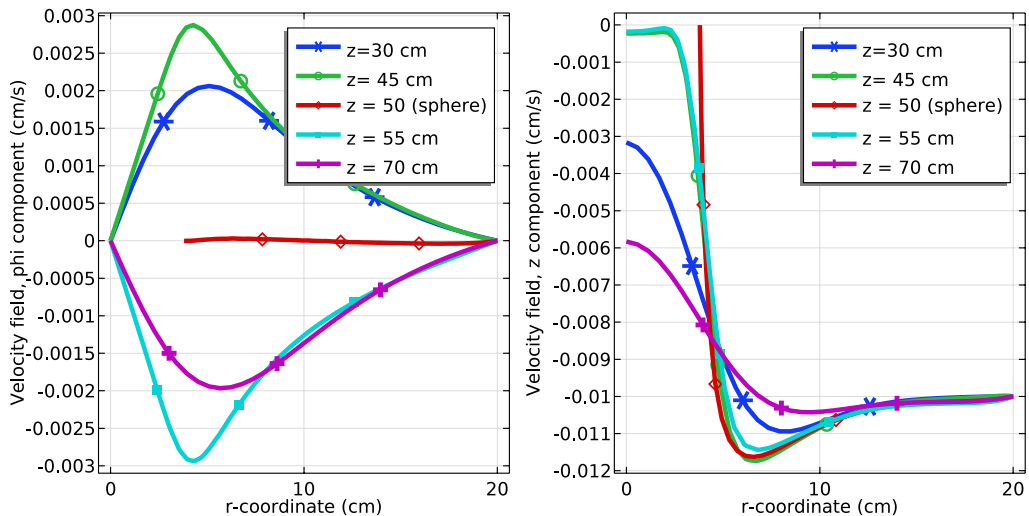


Figure 11: Plots of azimuthal velocity v_ϕ (left panel) and axial velocity v_r (right panel) vs. distance r from the central axis of the cylinder of Fig. 10, for an odd viscous liquid past a stationary sphere of radius 3.8 cm and located at elevation $z = 50$ cm. Each curve corresponds to a specific elevation in the cylinder where a probe has been placed. Two probes are located below the sphere at $z = 30$ and $z = 45$ cm, one lies at the level of the sphere ($z = 50$ cm) and two above the sphere at $z = 55$ and $z = 70$ cm. The left panel shows the counter-rotating azimuthal velocity components above and below the sphere as was also depicted in the left panel of Fig. 9. The magnitude of the azimuthal velocity decreases as one approaches the cylinder lids (at $z = 0$ and $z = 100$ cm) because liquid entering or leaving the cylinder has been set to have a vanishing azimuthal velocity component. The axial velocity of the liquid in the right panel shows similarities (and differences) with respect to the analogous flow of a fluid in a rotating cylinder as this was clearly described by Maxworthy (1970, Fig.7)

We find a velocity defect region (at $z = 70$ cm, cf. region I in the experiments of (Maxworthy 1970)) that is, the region where the velocity is less than the free stream one. This is surrounded by the region $5 < r < 15$, which has a velocity in excess of the free stream (region V in the experiments of (Maxworthy 1970)). The flow at $z = 30$ cm, is narrower and has larger axial velocity than its mirror counterpart (at $z = 70$ cm). Its angular velocity seems to be of the same magnitude compared with its mirror image (and this differs from the flow character in region VII of (Maxworthy 1970)).

The probe at $z = 55$ cm has a zero axial velocity close to the axis as this is determined by the Taylor-Proudman theorem, that the axial velocity of the slug is the same as the velocity of the body. The swirl however is nonzero and is actually quite large. This is region II in the experiments of (Maxworthy 1970). An Ekman layer induces a slow axial velocity where the surface of the sphere meets the anisotropy axis (close to $z = 45$ cm probe, and near $r = 0$). A sharp Ekman boundary-layer is seen to form at $z = 50$ cm, $r \sim 4$ cm.

We have not observed an oscillatory region downstream the sphere (region III of (Maxworthy 1970)) and we have not determined whether a region of clear fluid exists downstream and adjacent to the anisotropy axis.

The left panels of Figures 9 and 11 show the counterrotating character of the flow above and below the sphere, similar to Fig. 1 of Moore & Saffman (1968). The above discussion

displays an indirect verification for the validity of the Taylor-Proudman theorem in the case of odd viscous flow with a velocity field (v_r, v_ϕ, v_z) . v_z has the velocity of the body ($v_z = 0$), v_r is virtually zero and the flow outside the column is independent of z .

7. Vortex stretching and vortex twisting in a three-dimensional odd-viscous liquid.

The constitutive law (2.3) can be written in Cartesian coordinates in the form

$$\boldsymbol{\sigma}' = \eta_o \begin{pmatrix} -(\partial_x v + \partial_y u) & \partial_x u - \partial_y v & 0 \\ \partial_x u - \partial_y v & \partial_x v + \partial_y u & 0 \\ 0 & 0 & 0 \end{pmatrix}. \quad (7.1)$$

It is possible to define a modified pressure $\tilde{p} = p + \eta_o \zeta$ where $\zeta = \partial_x v - \partial_y u$ here is the component of vorticity in the z direction. Then, the odd Navier-Stokes equations are

$$\rho \frac{Du}{Dt} = -\partial_x \tilde{p} + \eta_o \partial_y (\partial_z w), \quad \rho \frac{Dv}{Dt} = -\partial_y \tilde{p} - \eta_o \partial_x (\partial_z w), \quad \rho \frac{Dw}{Dt} = -\partial_z \tilde{p} + \eta_o \partial_z \zeta. \quad (7.2)$$

What this equation shows is that vortex stretching $\partial_z w$ will be important on a region in the $x - y$ plane with vorticity ζ . To show this, let $\text{curl} \mathbf{v} = (\xi, \eta, \zeta)$ be the components of vorticity in Cartesian coordinates and consider a fluid particle whose vorticity points in the z direction instantaneously (we perform this to simplify the nonlinear term $\text{curl} \mathbf{u} \cdot \nabla \mathbf{v}$ that arises in the vorticity equation (3.27)). Taking the curl of (7.2), or considering directly the vorticity equation (3.27) we obtain

$$\frac{D\xi}{Dt} = (\zeta - \eta_o \nabla_2^2) \partial_z u, \quad \frac{D\eta}{Dt} = (\zeta - \eta_o \nabla_2^2) \partial_z v, \quad \frac{D\zeta}{Dt} = (\zeta - \eta_o \nabla_2^2) \partial_z w. \quad (7.3)$$

Thus, the well-known vortex twisting, represented by the quantities $\partial_z u$ and $\partial_z v$ (cf. (Tritton 1988, §6.6)) is now enhanced by the extra term $\eta_o (k_x^2 + k_y^2)$ appearing in the round brackets in Eq. (7.3) induced by odd viscosity. Likewise, vortex stretching, represented by the quantity $\partial_z w$ is also enhanced by odd viscosity.

Of course, for a two-dimensional incompressible odd viscous liquid where the velocity does not depend on z , we have

$$\frac{D\zeta}{Dt} = 0, \quad (7.4)$$

as is also known from the ‘‘absorption’’ of the odd viscous force density into the pressure gradient, see eg. (Ganeshan & Abanov 2017), and thus the vorticity of a fluid particle in a two-dimensional odd viscous liquid is conserved.

8. The effect of the η_4 odd viscous stress tensor

Referring to the stress tensor (2.2), in this article we tacitly assumed that only the coefficient η_3 was nonvanishing which led the odd stress tensor to acquire the form (7.1) in Cartesian coordinates. The coefficient η_4 in (2.2) gives rise however to an additional odd stress tensor. In this section we discuss the consequences of the latter, in the context of the effects developed in this article.

As in section 2 we consider the field \mathbf{b} to lie in the z -direction. Then, the odd stress tensor acquires the additional components

$$\boldsymbol{\sigma}' = \eta_4 \begin{pmatrix} 0 & 0 & -(\partial_y w + \partial_z v) \\ 0 & 0 & \partial_x w + \partial_z u \\ -(\partial_y w + \partial_z v) & \partial_x w + \partial_z u & 0 \end{pmatrix}, \quad (8.1)$$

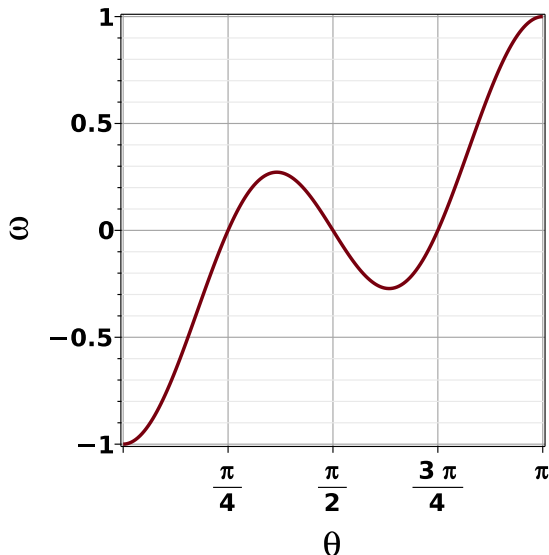


Figure 12: Plane-polarized wave dispersion ω (Eq. (8.7)) versus angle θ between the wavevector \mathbf{k} and the z - (anisotropy) axis (setting $k = -\nu_4 = 1, \nu_o = 0$). It differs qualitatively from its $\eta_o \neq 0$ counterpart displayed in Fig. 6 by crossing the $\omega = 0$ axis at angles different than $\pi/2$ and by displaying additional inflection points which signal that the maxima of group velocity may appear at angles that differ to $\pi/2$.

where we adopted the opposite sign to (Lifshitz & Pitaevskii 1981, Eq. (58.16)). We proceed below to examine the form of inertial-like waves in an odd viscous liquid whose constitutive law is the combination of (7.1) and (8.1).

8.1. Plane-polarized waves

We define the linear operator

$$\mathcal{S} = (\nu_o - \nu_4)\nabla_2^2 + \nu_4\partial_z^2, \quad (8.2)$$

where $\nu_4 = \eta_4/\rho$ and $\nabla_2^2 = \partial_x^2 + \partial_y^2$. To obtain an understanding of the effect odd viscosity parameters have on the type of solutions we classify the operator \mathcal{S} in (8.2) as follows

- \mathcal{S} is elliptic when $\nu_o > \nu_4$.
- \mathcal{S} is hyperbolic when $\nu_o < \nu_4$.
- \mathcal{S} is parabolic when $\nu_o = \nu_4$.

Here we have assumed that z plays the role of the time-like variable. This is the standard route followed in rigidly-rotating liquids, see (Whitham 1974, §12.6).

With the notation $\zeta = \partial_x v - \partial_y u$ for the component of vorticity in the z direction and a modified pressure $\tilde{p} = p + \eta_4\zeta$, the Navier-Stokes equations (3.26) are replaced by

$$\frac{D\mathbf{v}}{Dt} = -\frac{1}{\rho}\nabla\tilde{p} + \mathcal{S}\hat{\mathbf{z}} \times \mathbf{v}, \quad (8.3)$$

and the vorticity equation (3.28) by

$$\partial_t \text{curl} \mathbf{v} = -\mathcal{S} \frac{\partial \mathbf{v}}{\partial z}. \quad (8.4)$$

With $\mathbf{v} = \mathbf{A}e^{i(\mathbf{k}\cdot\mathbf{r}-\omega t)}$ the vorticity equation (8.4) becomes a system of three equations

for the three unknown components of the amplitude \mathbf{A} . This system has a nontrivial solution when the determinant of the matrix

$$\begin{pmatrix} -ik_z \mathcal{S}(\mathbf{k}) & \omega k_z & -\omega k_y \\ -\omega k_z & -ik_z \mathcal{S}(\mathbf{k}) & \omega k_x \\ \omega k_y & -\omega k_x & -ik_z \mathcal{S}(\mathbf{k}) \end{pmatrix} \quad (8.5)$$

vanishes. Here,

$$\mathcal{S}(\mathbf{k}) = -(\nu_o - \nu_4)(k_x^2 + k_y^2) - \nu_4 k_z^2. \quad (8.6)$$

The dispersion relation becomes

$$\omega = \mp \mathcal{S}(\mathbf{k}) \frac{k_z}{k} \quad \text{or} \quad \omega = \pm \cos(\theta) k^2 [\nu_o - \nu_4 - (\nu_o - 2\nu_4) \cos^2 \theta]. \quad (8.7)$$

Here and below the reader can keep in mind the parabolic case $\nu_o = \nu_4$ and the elliptic case $\nu_o = 2\nu_4$ (parabolic and elliptic with respect to the operator \mathcal{S} in (8.2)) which simplify all relations significantly and are to be discussed in what follows.

We display the dispersion Eq. (8.7) for $\nu_o = 0$ in Fig. 12, to be compared with Fig. 6. This dispersion relation is interesting as it crosses the $\omega = 0$ axis at angles $\theta = \pi/4$ (different to the $\pi/2$ of rigidly-rotating liquids or the η_o odd viscous liquid). Likewise, it has an inflection point at $\theta \neq \pi/2$, which signals the presence of a maximum for the group velocity that differs to the ones of rigidly-rotating liquids and the η_o odd viscous liquid. The group velocity (3.36) is replaced by

$$\left(\frac{\partial \omega}{\partial k_x}, \frac{\partial \omega}{\partial k_y} \right) = \pm k ((\nu_o - 2\nu_4) \cos^2 \theta + \nu_o - \nu_4) \sin \theta \cos \theta (\cos \phi, \sin \phi), \quad (8.8)$$

$$\frac{\partial \omega}{\partial k_z} = \pm k ((\nu_o - 2\nu_4) \cos^4 \theta + (-2\nu_o + 5\nu_4) \cos^2 \theta + \nu_o - \nu_4), \quad (8.9)$$

with modulus

$$|c_g| = k \left[-5(\nu_o - 2\nu_4)^2 \cos^6 \theta + (7\nu_o - 16\nu_4)(\nu_o - 2\nu_4) \cos^4 \theta \right. \quad (8.10)$$

$$\left. -3(\nu_o - \nu_4)(\nu_o - 3\nu_4) \cos^2 \theta + (\nu_o - \nu_4)^2 \right]^{1/2}. \quad (8.11)$$

Its components and modulus are displayed in Fig. 13 for the case $\nu_o = 0$. The modulus of the group velocity displays a maximum at $\theta \neq \pi/2$ as expected from the properties of the corresponding dispersion relation (8.7).

When the flow field is determined by the plane-polarized waves $\mathbf{v} = \mathbf{A} e^{i(\mathbf{k} \cdot \mathbf{r} - \omega t)}$ considered in this section, its helicity is conserved for an odd viscous liquid that incorporates both constitutive laws (7.1) and (8.1). That is the case because in wave-number and frequency-space the linearized vorticity equation (8.4) can be written in the form

$$-i\omega \mathbf{B} = -i\mathbf{A} k_z \mathcal{S}(\mathbf{k}), \quad (8.12)$$

when $\text{curl} \mathbf{v} = \mathbf{B} e^{i(\mathbf{k} \cdot \mathbf{r} - \omega t)}$ and $\mathcal{S}(\mathbf{k})$ is defined in Eq. (8.6). Since $\omega = \mp \mathcal{S}(\mathbf{k}) \frac{k_z}{k}$ (from (8.7)) we obtain $\mathbf{B} = \mp k \mathbf{A}$, or

$$\text{curl} \mathbf{v} = \mp k \mathbf{v}. \quad (8.13)$$

Thus, the helicity of the flow field determined by the odd stress tensors (7.1) and (8.1) is conserved

$$\mathbf{v} \cdot \text{curl} \mathbf{v} = \mp k |\mathbf{v}|^2. \quad (8.14)$$

In addition, $\mathbf{c}_g \cdot \mathbf{c}_p = 2 [(\nu_o - 2\nu_4) \cos^2 \theta - \nu_o + \nu_4]^2 k^2 \cos^2 \theta = 2|\mathbf{c}_p|^2$, so the last two lines of Table 1 remain unchanged.

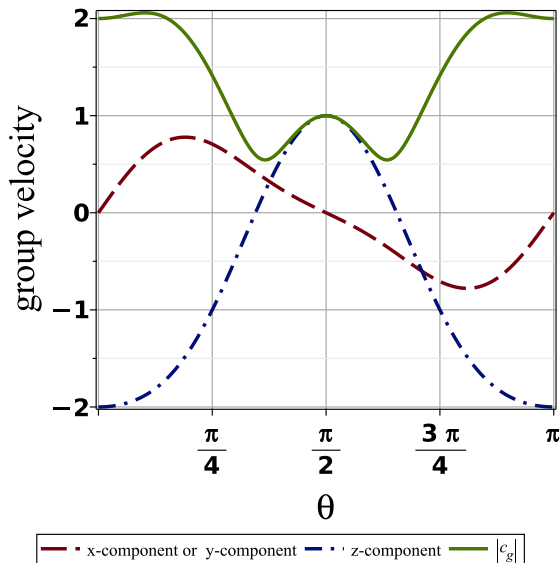


Figure 13: Group velocity components (8.8) and magnitude versus angle θ between the wavevector \mathbf{k} and the z - (anisotropy) axis, setting $k = -\nu_4 = 1, \nu_o = 0$ (and $\phi = \pi/4$, for simplicity). The magnitude develops maxima at angles $\theta \neq \pi/2$, differing to those of the rigidly-rotating liquid or the η_o odd viscous liquid, cf. Fig. 8.

Equation (8.3) can be employed to investigate the possibility of Taylor column formation in an odd viscous liquid that incorporates the stress tensor (7.1) and (8.1). Dropping the left-hand side of (8.3), it reads, in component form

$$\frac{1}{\rho} \frac{\partial \tilde{p}}{\partial x} = -\mathcal{S}v, \quad \frac{1}{\rho} \frac{\partial \tilde{p}}{\partial y} = \mathcal{S}u, \quad \frac{\partial \tilde{p}}{\partial z} = 0, \quad (8.15)$$

and carrying-out the same manipulations as in section 5 we obtain the conditions

$$\partial_z \mathcal{S}u = \partial_z \mathcal{S}v = \partial_z \mathcal{S}w = 0, \quad \text{and} \quad \partial_x \mathcal{S}u + \partial_y \mathcal{S}v = 0, \quad (8.16)$$

which replace (5.6). The form of both equations (8.15) and (8.16) is appealing and resembles (5.1) and (5.6), respectively. They still lead to Taylor column-like structures which however are not identical to those of rigidly-rotating liquids.

In Fig. 14 we repeat the simulations of Fig. 9 now with vanishing odd viscosity η_o and $\eta_4 = 1 \text{ g}/(\text{cm sec})$. On the right panel of Fig. 14 we observe a column circumscribing the sphere. It does not have the characteristics of a Taylor column present in rigidly-rotating liquids (where w is equal to the velocity of the body circumscribed by the column). Here the variation of w with respect to z , away from boundaries, is mostly of the form of a lower degree polynomial in z plus some oscillatory behavior of low amplitude. This behavior is expected from the form of governing equation $\partial_z \mathcal{S}w = 0$ in (8.16). Its particular solution is some quadratic polynomial (at most) in z to which one can superpose the solution of the homogeneous problem which is oscillatory in z .

The left panel of Fig. 14 shows additional lobes of azimuthal velocity. This agrees with the observations of (Khain *et al.* 2022, Fig.4(d)) for the analogous problem in Stokes flow. There are regions where the sense of rotation changes with distance from the axis, i.e. the azimuthal velocity lobes that are additional to the ones of Fig. 9.

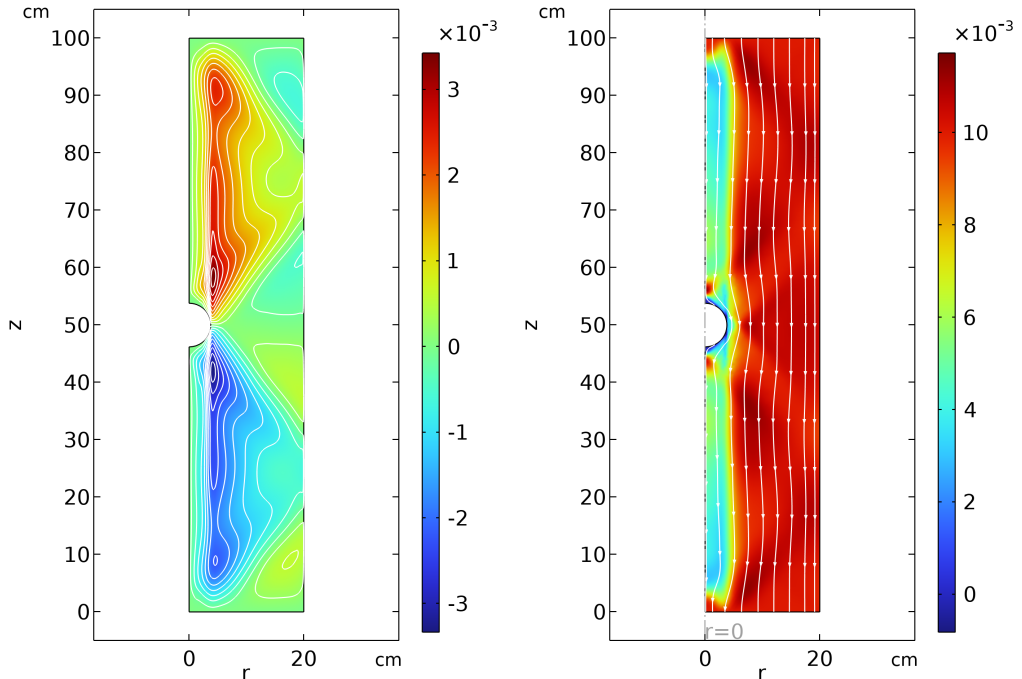


Figure 14: Distribution of azimuthal (left panel) and axial velocity (right panel) in an odd viscous liquid described by the constitutive law (8.1) ($\eta_o = 0$ and $\eta_4 = 1$ g/(cm sec)), moving slowly and meeting an immobile sphere (of radius 3.8 cm) located at elevation $z = 50$ cm at the center axis of a cylinder. Liquid enters from the top ($z = 100$ cm) and exits at the bottom ($z = 0$). The sphere is not allowed to rotate. **Left:** Counter-rotation of liquid takes place above and below the sphere in the azimuthal direction. As observed in (Khain *et al.* 2022, Fig.4(d)) for the analogous problem in Stokes flow, there are regions where the sense of rotation changes with distance from the axis, i.e. the azimuthal velocity lobes that are additional to the ones of Fig. 9. **Right:** A column whose generators are parallel to the cylinder axis and circumscribes the sphere is also visible in the right panel.

8.2. Axisymmetric inertial-like waves when $\eta_o \equiv 0$

We express the constitutive law (8.1) in cylindrical coordinates

$$\boldsymbol{\sigma}' = \eta_4 \begin{pmatrix} 0 & 0 & -\left(\frac{1}{r}\partial_\phi v_z + \partial_z v_\phi\right) \\ 0 & 0 & \partial_r v_z + \partial_z v_r \\ -\left(\frac{1}{r}\partial_\phi v_z + \partial_z v_\phi\right) & \partial_r v_z + \partial_z v_r & 0 \end{pmatrix} \quad (8.17)$$

and repeat the construction of axial waves of section 3.4. The linearized equations of motion (see Appendix B) become

$$-i\omega v_r = -\frac{1}{\rho} \frac{\partial p'}{\partial r} + \nu_4 k^2 v_\phi, \quad (8.18)$$

$$-i\omega v_\phi = -\nu_4 \left[\frac{1}{r} \frac{\partial}{\partial r} \left(r \frac{\partial v_r}{\partial r} \right) - \frac{v_r}{r^2} \right] - \nu_4 k^2 v_r, \quad (8.19)$$

$$-i\omega v_z = -\frac{ik}{\rho} p' - ik\nu_4 \frac{1}{r} \frac{\partial}{\partial r} (r v_\phi), \quad (8.20)$$

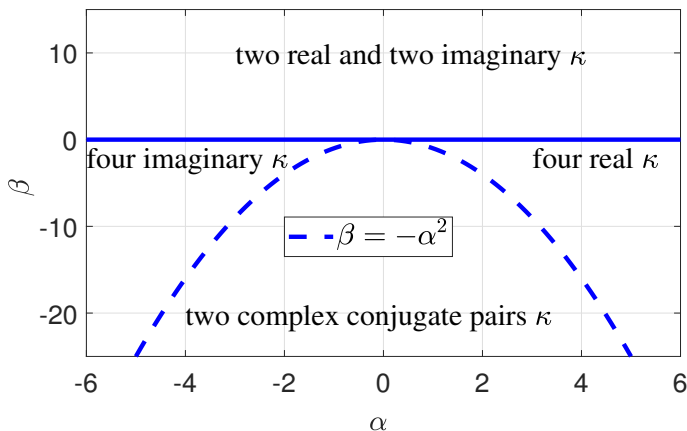


Figure 15: Behavior of roots κ of Eq. (8.27) & (8.29) in the parameter space (α, β) defined in Eq. (8.28). This includes the oscillatory Bessel functions for real κ , exponentially increasing/decreasing Bessel functions for κ imaginary and exponential-oscillating Bessel functions for complex κ .

where we simplified (8.19) by employing the incompressibility condition (3.4). Introducing the linear operator (3.5) $\mathcal{L} = \partial_r^2 + \frac{1}{r}\partial_r - \frac{1}{r^2}$ the r and ϕ momentum equations become

$$-i\omega v_r = -i\frac{\omega}{k^2}\mathcal{L}v_r + \nu_4(\mathcal{L} + k^2)v_\phi, \quad (8.21)$$

$$-i\omega v_\phi = -\nu_4(\mathcal{L} + k^2)v_r. \quad (8.22)$$

It is clear that the structure of these equations is identical to (3.6) and (3.7) with the exception of the k^2 terms in the round brackets. The velocities v_r and v_ϕ are again the Bessel functions, $v_r = AJ_1(\kappa r)$, $v_\phi = BJ_1(\kappa r)$ (considering only the case where the origin is included in the domain). System (8.21) and (8.22) has a solution when the determinant $-\kappa^4 k^2 \nu_4^2 + (2k^4 \nu_4^2 + \omega^2) \kappa^2 - k^2 (k^2 \nu_4 - \omega) (k^2 \nu_4 + \omega)$ of the coefficients of the resulting linear system vanishes (for a derivation see Eq. (8.26)). For real ω and k , κ satisfies

$$\kappa^2 = \frac{\omega^2 + 2k^4 \nu_4^2 \pm \omega \sqrt{8k^4 \nu_4^2 + \omega^2}}{2k^2 \nu_4^2}. \quad (8.23)$$

There are two imaginary and two real roots when $\omega^2 - \nu_4^2 k^4 > 0$. There are four real κ roots in (8.23) when $\omega^2 - \nu_4^2 k^4 < 0$ (the derivation of both is discussed below and summarized in Table 2). This is to be expected from the form of the operator \mathcal{S} in (8.2) that determines the character of solutions. In contrast, in case (3.9) there are two real and two imaginary roots. Solving (8.23) for ω one recovers (8.7) with $k_x^2 + k_y^2$ replaced by κ^2 .

8.3. Combined effect of η_4 and η_o on axisymmetric inertial-like waves

It turns out that a richer behavior is present when both η_o and η_4 stress tensors (2.3) and (8.17) are considered. Superposing the right hand sides of (3.1)-(3.3) to (8.18)-(8.20) and carrying-out the same manipulations as above with the same linear operator (3.5)

$\mathcal{L} = \partial_r^2 + \frac{1}{r}\partial_r - \frac{1}{r^2}$, the r and ϕ momentum equations become

$$-i\omega v_r = -i\frac{\omega}{k^2}\mathcal{L}v_r + \nu_4(\mathcal{L} + k^2)v_\phi - \nu_o\mathcal{L}v_\phi, \quad (8.24)$$

$$-i\omega v_\phi = -\nu_4(\mathcal{L} + k^2)v_r + \nu_o\mathcal{L}v_r. \quad (8.25)$$

System (8.24) and (8.25) has a solution when the determinant $-(\nu_o - \nu_4)^2 k^2 \kappa^4 + (-2k^4\nu_o\nu_4 + 2k^4\nu_4^2 + \omega^2)\kappa^2 - k^2(k^2\nu_4 - \omega)(k^2\nu_4 + \omega)$ of the coefficients of the resulting linear system

$$\frac{iBk^4\nu_4 + i(\nu_o - \nu_4)\kappa^2 Bk^2 - A\kappa^2\omega}{k^2\omega} - A = 0, \quad \text{and} \quad -\frac{iA((\nu_o - \nu_4)\kappa^2 + k^2\nu_4)}{\omega} - B = 0 \quad (8.26)$$

vanishes. The velocity field is again expressed with respect to Bessel functions $v_r = AJ_1(\kappa r)$ and $v_\phi = BJ_1(\kappa r)$. For real ω and k the eigenvalue κ is

$$\kappa^2 = \frac{\pm\omega\sqrt{4(\nu_o - \nu_4)(\nu_o - 2\nu_4)k^4 + \omega^2} + \omega^2 - 2k^4\nu_4(\nu_o - \nu_4)}{2(\nu_o - \nu_4)^2 k^2}. \quad (8.27)$$

To understand the structure of solutions we define the frequency squared parameter α and quartic power of frequency β of the form

$$\alpha = \omega^2 + 2k^4\nu_4(\nu_4 - \nu_o), \quad \beta = 4k^4(\nu_o - \nu_4)^2(\omega^2 - \nu_4^2 k^4). \quad (8.28)$$

With this notation Eq. (8.27) simplifies to

$$2(\nu_o - \nu_4)^2 k^2 \kappa^2 = \alpha \pm \sqrt{\alpha^2 + \beta}. \quad (8.29)$$

In Fig. 15 we display all possible κ behaviors inherent in (8.27) and (8.29) and two cases are summarized in Table 2. Thus, referring to Fig. 15, when $\eta_4 \equiv 0$, β is positive and there are two real and two imaginary roots κ (case considered in section 3.4). When $\eta_o \equiv 0$ (this is the case (8.23)), α is always positive and $\alpha^2 + \beta > 0$. Thus, when $\beta < 0$ there are four real κ roots. In the opposite case two imaginary and two real. In the elliptic case $\eta_o = 2\eta_4$ there can be four imaginary or two imaginary and two real κ , as this case is tabulated in Table 2. The fact that the operator \mathcal{S} in (8.2) is hyperbolic when $\nu_o = 0$ and elliptic when $\nu_o = 2\nu_4$ is clearly reflected in the type of roots κ and thus the form of the velocity field.

Finally, of interest might also be the parabolic case where $\nu_o = \nu_4$. This case is separate from (8.27) since the equations determining κ are of second order in spatial derivatives (they are fourth order in the case (8.27)). We obtain

$$\kappa^2 = \frac{(k^4\nu_4^2 - \omega^2)k^2}{\omega^2}, \quad (8.30)$$

giving rise to either two real κ or two imaginary κ . The dispersion relation reads

$$\omega = \pm \frac{\nu_4 k^3}{\sqrt{\kappa^2 + k^2}}. \quad (8.31)$$

9. Comparison to the recent literature of odd viscous liquids

We conclude this paper by summarizing a few results, taken from the recent literature, that are related to the present paper, where some of them also appeared in the foregoing analysis.

Consider the joint η_o and η_4 effects. The identification $\eta_o = 2\eta_4$ has been employed

	$\omega^2 < \nu_4^2 k^4 \mid \nu_4^2 k^4 < \omega^2 < 2\nu_4^2 k^4 \mid \omega^2 > 2\nu_4^2 k^4$		
$\eta_o = 0$	$\begin{array}{c} \alpha \\ \beta \\ \kappa \end{array}$	$\begin{array}{c} + \\ - \\ 4 \text{ Re} \end{array}$	$\begin{array}{c} + \\ + \\ 2 \text{ Im} + 2 \text{ Re} \end{array}$
$\eta_o = 2\eta_4$	$\begin{array}{c} \alpha \\ \beta \\ \kappa \end{array}$	$\begin{array}{c} - \\ - \\ 4 \text{ Im} \end{array}$	$\begin{array}{c} - \\ + \\ 2 \text{ Im} + 2 \text{ Re} \end{array}$

Table 2: Types of roots κ from Eq. (8.27)/(8.29) where $\kappa^2 \propto \alpha \pm \sqrt{\alpha^2 + \beta}$ according to the sign of the parameters α and β defined in Eq. (8.28) for two special choices of the odd viscosity parameters. In all cases $\alpha^2 + \beta > 0$. Re = Real κ . Im = Imaginary κ .

in the literature as a means to incorporate effects of both odd coefficients η_o and η_4 and to simplify the presentation (Khain *et al.* 2022). The dispersion relation (8.7) $\omega = -k^2 ((\nu_o - 2\nu_4) \cos^2 \theta - \nu_o + \nu_4) \cos \theta$ simplifies significantly giving

$$\omega = \nu_4 k k_z, \quad (9.1)$$

which recovers the dispersion relation of a Hamiltonian formulation of spinning molecules (Markovich & Lubensky 2021, Eq. (8)).

As discussed above, the counter-rotation of an odd viscous liquid below and above a slowly-moving sphere in Fig. 9 ($\eta_o \neq 0, \eta_4 = 0$) agrees with the observations of (Khain *et al.* 2022, Fig.4(c)) for the analogous problem in Stokes flow. Similarly, the presence of additional lobes of azimuthal velocity in Fig. 9 ($\eta_o = 0, \eta_4 \neq 0$), was also observed in Stokes flow (Khain *et al.* 2022, Fig.4(d)).

In general, large values of the odd viscosity lead to recirculating patterns, see (Khain *et al.* 2022, Fig. 6(h)) in agreement with the restoring effect of an odd viscous liquid discussed in the introduction of the present paper. The combination $\eta_o = 2\eta_4$ leads to swirling flow with a large azimuthal velocity component. This type of flow is stabilizing. Thus, we can say for instance that a cloud sedimenting in an odd viscous liquid (Khain *et al.* 2022, Fig. 6(b)) is circumscribed by its own Taylor column and it does not disintegrate.

10. Discussion

In this article we showed that inertial-like waves and Taylor columns are generated in a three-dimensional odd viscous liquid. Both odd coefficients η_o and η_4 that appear in the constitutive laws (7.1) and (8.1) are nicely tucked-away in a compact differential operator \mathcal{S} Eq. (8.2) and result in the odd form of the Navier-Stokes equations (8.3) and (8.4). The flow that arises from the consideration of plane-polarized waves is a Beltrami flow. Thus, its helicity is conserved. The flow field determined by three dimensional axisymmetric waves in an odd η_o and η_4 liquid has a structure that is determined by the eigenvalues κ in the argument of the Bessel function $J_1(\kappa r)$ (or $Y_1(\kappa r)$) and a classification of different behaviors is displayed in Fig. 15. Thus, the velocity field can be oscillatory, exponential increasing/decaying or their combination thereof.

Considering the behavior of liquids with a single η_o odd viscosity coefficient, we can isolate two important results that were developed here. First, we observe inertial oscillations downstream a slowly moving body whose theoretically determined wavelength

Eq. (3.22) is in agreement with its estimate from solutions of the full Navier-Stokes equations (in an analogous manner to the experiments of Long (1953) which were in agreement with the theory of inertial oscillations in rigidly rotating liquids, cf. (Batchelor 1967, plate 24)). Second, we observe Taylor-column-like behavior when a sphere slowly moves along the axis of anisotropy, and this also resembles the behavior of a rigidly-rotating liquids, for instance, in the experiments of Maxworthy (1970). The latter behavior is to be expected since, when the wavevector is perpendicular to the anisotropy axis, the flow becomes effectively two-dimensional in agreement with the (modified) Taylor-Proudman theorem we developed here, suitable for odd viscous liquids. At the same time helicity segregation signals the generation of inertial-like waves at the interior of the column where information is transported along the anisotropy axis, above the body and below the body at the group velocity.

Our theoretical discussion was predominantly centered on an odd viscous liquid with zero shear viscosity (in the numerical simulations of the Navier-Stokes equations shear viscosity was however, small but non-zero). Shear viscosity would just endow the frequency ω with an imaginary part, as is the case in rigidly-rotating liquids, see for instance (Chandrasekhar 1961, p. 86, Eq. (72)).

There is a large number of unexplored phenomena in three-dimensional odd viscous liquids associated with the findings in this paper. To name a few, what is the effect of shear viscosity on Taylor columns, and thus the establishment of Ekman and Stewartson layers. The effect of different flow conditions (eg. flow incident on a finite length obstacle also generating Taylor columns), the effect of different material properties (eg. a liquid droplet instead of a solid sphere rising slowly in such a liquid, cf. (Bush *et al.* 1994, 1995)), a freely suspended sphere rising slowly in such a liquid and finally an experimental realization of these effects. Also, determination of criteria for Taylor-column formation in bounded and unbounded domains. To understand the diversity behind these issues in the case of rotating liquids, one can be apprised by the review of Bush *et al.* (1994).

The formulation developed in this paper can prove to be useful in many areas of research. For instance, one could envision the following application of odd viscous liquid Taylor columns to materials science: Semiconducting nanowires, employed in diverse fields such as biological molecule sensing and living cell probing, are manufactured by the vapor-liquid-solid growth technique, whereby a liquid-alloy droplet increases in size by absorbing material from a vapor phase. Hydrodynamics has been shown to be an important factor in this process (Schwalbach *et al.* 2012). Disruption of growth may take place in the form of instabilities leading the nanowire to adopt distorted shapes or to develop random extrusions. These instability mechanisms may however become suppressed in the presence of odd viscosity. Slow impinging flow on a nanowire will circumscribe each one of them to its own Taylor column, thus providing a unidirectional guide for droplet-alloy growth, circumventing the generation of instabilities. Thus, a fundamental related open question concerns the effect odd viscosity has on convection.

Acknowledgments

This research was supported by the Center for Bio-Inspired Energy Science, an Energy Frontier Research Center funded by the US Department of Energy, Office of Science, Basic Energy Sciences under Award No. DE-SC0000989. We thank Leticia Lopez and four anonymous referees for comments that improved the manuscript.

Declaration of Interests

The authors report no conflict of interest.

Appendix A. Odd viscous stress

In two dimensions it has been shown (Kirkinis *et al.* 2022) that the odd viscous stress tensor and thus the total stress, can succinctly be written in the form

$$\boldsymbol{\sigma} = -p\mathbf{I} + 2 \begin{pmatrix} \eta_e & -\eta_o \\ \eta_o & \eta_e \end{pmatrix} D, \quad (\text{A } 1)$$

in terms of the two-dimensional rate-of-strain tensor

$$D_{ij} = \frac{1}{2} \left(\frac{\partial u_i}{\partial x_j} + \frac{\partial u_j}{\partial x_i} \right), \quad i, j = 1, 2 \quad (\text{A } 2)$$

for an incompressible liquid. Expression (A 1) is important because it clarifies the origin of physical effects appearing on a free surface of an odd viscous liquid. In this section we would like to obtain an analogous expression for the three dimensional odd viscous stress (7.1) and (8.1). To this end, define the three dimensional rotation matrix

$$R = \begin{pmatrix} 0 & -1 & 0 \\ 1 & 0 & 0 \\ 0 & 0 & 0 \end{pmatrix} \quad (\text{A } 3)$$

so that $R^T = -R$. A little work (using the notation $\sigma^o = 2\eta_o \begin{pmatrix} -D_{12} & \frac{D_{11}-D_{22}}{2} & 0 \\ \frac{D_{11}-D_{22}}{2} & D_{12} & 0 \\ 0 & 0 & 0 \end{pmatrix}$

etc. here D_{ij} should be understood as the upper left two by two block of the three-dimensional rate-of-strain tensor) shows that

$$\sigma^o = \eta_o [RD + (RD)^T] = \eta_o [RD - DR]. \quad (\text{A } 4)$$

We can repeat the above for the tensor (8.1) (here D should be understood as the rate-of-strain tensor without the upper left two by two block) and obtain

$$\sigma^4 = \eta_4 [RD + (RD)^T] = \eta_4 [RD - DR]. \quad (\text{A } 5)$$

When $\eta_o = \eta_4$ (this is the parabolic case for the operator \mathcal{S} of section 8) we can employ a compact notation for the stress tensor incorporating both odd coefficients and the shear viscosity η_e by splitting the even stress tensor $\sigma^e = 2\eta_e D = \eta_e (ID + DI)$, where I is the unit matrix to obtain

$$\boldsymbol{\sigma} = -p\mathbf{I} + (\eta_e I + \eta_o R)D + D(\eta_e I - \eta_o R), \quad (\text{A } 6)$$

where D is the three-dimensional rate-of-strain tensor

$$D_{ij} = \frac{1}{2} \left(\frac{\partial u_i}{\partial x_j} + \frac{\partial u_j}{\partial x_i} \right), \quad i, j = 1, 2, 3. \quad (\text{A } 7)$$

Alternatively, define the viscosity matrix

$$\hat{\eta} = \begin{pmatrix} \eta_e & -\eta_o & 0 \\ \eta_o & \eta_e & 0 \\ 0 & 0 & \eta_e \end{pmatrix} \quad (\text{A } 8)$$

Then, the full stress tensor in three dimensions obtains the form

$$\boldsymbol{\sigma} = -p\mathbf{I} + \hat{\eta}D + D\hat{\eta}^T, \quad (\text{A } 9)$$

which is the analogue of (A 1). In two dimensions $D_{11} = -D_{22}$ and Eq. (A 9) immediately reduces to Eq. (A 1).

One immediate consequence of writing the odd stress tensor in the form (A 4) or (A 5) is that it makes clear the effect of odd viscosity on dissipation of energy. The kinetic energy density (Landau & Lifshitz 1987, §16)

$$\dot{E}_{\text{kin}} = -\text{tr}(\sigma^o D)$$

vanishes immediately since σ^o in (A 4) is the product of a symmetric and an antisymmetric matrix (tr denotes the trace of a matrix), and likewise for σ^4 .

Appendix B. Linearized equations of motion

$$\partial_t v_r = -\frac{1}{\rho} \frac{\partial p'}{\partial r} + \frac{1}{\rho} \left[\frac{1}{r} \partial_r (r \sigma_{rr}) + \frac{1}{r} \partial_\phi \sigma_{r\phi} + \partial_z \sigma_{rz} - \frac{1}{r} \sigma_{\phi\phi} \right], \quad (\text{B1})$$

$$\partial_t v_\phi = -\frac{1}{\rho r} \frac{\partial p'}{\partial \phi} + \frac{1}{\rho} \left[\frac{1}{r^2} \partial_r (r^2 \sigma_{\phi r}) + \frac{1}{r} \partial_\phi \sigma_{\phi\phi} + \partial_z \sigma_{\phi z} + \frac{1}{r} (\sigma_{r\phi} - \sigma_{\phi r}) \right], \quad (\text{B2})$$

$$\partial_t v_z = -\frac{1}{\rho} \frac{\partial p'}{\partial z} + \frac{1}{\rho} \left[\frac{1}{r} \partial_r (r \sigma_{zr}) + \frac{1}{r} \partial_\phi \sigma_{z\phi} + \partial_z \sigma_{zz} \right]. \quad (\text{B3})$$

Note that the definition of the stress tensor in fluid mechanics (cf. (Landau & Lifshitz 1987)) differs from its definition in the continuum mechanics literature where it is defined as the transpose. Here we follow the fluid mechanics notation, as this arises for instance in (Landau & Lifshitz 1987).

Appendix C. Basic facts about rotating fluids

The Rossby and Ekman numbers are

$$Ro = \frac{U}{\Omega L}, \quad E = \frac{\nu}{\Omega L}. \quad (\text{C1})$$

In the axisymmetric case where $\partial_\phi = 0$, the Taylor-Proudman theorem for the geostrophic equations

$$-\Omega v_\phi = -\frac{1}{\rho} \frac{\partial p}{\partial r}, \quad \Omega v_r = 0, \quad 0 = \frac{\partial p}{\partial r} \quad (\text{C2})$$

implies that $v_r \equiv 0$ and thus the streamlines are spirals that wound around circular cylinders (Yih 1959).

C.1. Taylor columns

The geostrophic equations, in Cartesian coordinates, written in the form

$$\frac{1}{\rho} \frac{\partial p}{\partial x} = -\Omega v, \quad \frac{1}{\rho} \frac{\partial p}{\partial y} = \Omega u, \quad \frac{\partial p}{\partial z} = 0, \quad (\text{C3})$$

show that the pressure p is a streamfunction and thus constant on a streamline of the flow. A finite-length cylinder with generators parallel to the rotating axis and moving horizontally in a rotating liquid will thus be accompanied by a liquid velocity parallel to its generators and a column will accompany its motion (Yih 1988, §12.2). Inside the column the velocity can be zero, although viscous liquids are accompanied with special flows where the velocity does not vanish (Moore & Saffman 1968).

Separate two-dimensional flows exist inside and outside the Taylor column. Liquid cannot be transferred between these two regions. This is clear in the axisymmetric case

where v_r vanishes everywhere (outside the Taylor column). Experimentally dye that is outside the Taylor column cannot enter and dye inside does not exit (Tritton 1988, Fig.16.2). The flow inside the Taylor column is determined by taking into account the thin shear layers that develop on the lateral surface of the Taylor column and the Ekman boundary-layers on the body and the boundaries (Moore & Saffman 1968).

C.2. Elasticity induced by rotation of an inviscid liquid

Consider a particle of unit mass that moves with a speed v perpendicular to the axis of rotation. Momentum conservation gives

$$\frac{v^2}{r} = 2\Omega v. \quad (\text{C } 4)$$

Solving for r we obtain $r = \frac{v}{2\Omega}$. This implies that the locus of the particle is a circle. It goes around the circle twice during every revolution of the liquid with period $T = 2\pi r/v = \pi/\Omega$ (the vorticity of the liquid in rigid-body rotation is twice the angular velocity of rotation) (Tritton 1988, §16.6).

The effect of this constraining tendency is to support inertial waves. As remarked above, inertial waves exist only when $\omega < 2\Omega$ since $\kappa = k\sqrt{\frac{4\Omega^2}{\omega^2} - 1}$ must be real.

The relations (Taylor-Proudman theorem)

$$\frac{\partial u}{\partial z} = \frac{\partial v}{\partial z} = 0, \quad (\text{C } 5)$$

do not allow vortex twisting (the liquid velocity approaching a finite obstacle does not change relative to the obstacle - vorticity is not generated), see (Tritton 1988, Fig.16.5). This means that the background vorticity resists twisting. On the other hand the condition

$$\frac{\partial w}{\partial z} = 0, \quad (\text{C } 6)$$

resists vortex stretching (vortex tubes do not thin to increase vorticity see (Tritton 1988, Fig.16.6)).

Another view of the same effect is to displace a circular ring of fluid outward to a new position r . The circulation $2\pi vr$ along that ring remains the same according to Kelvin's theorem. Thus, the ring's v and v^2/r will be smaller to the new position. However the liquid v^2/r was larger there and it was balanced exactly by a pressure gradient, which, now sees the lower v^2/r of the ring. Thus, it will push the ring back towards its original position. The pressure at this position will push it again outwards and the ring will experience an oscillatory motion (Yih 1988, §5). See also (Davidson 2013, Chapter 1) for a more detailed explanation of the same effect. A similar discussion about the restoring effect of the Coriolis force can be traced back to (Batchelor 1967, §7.6).

REFERENCES

- ABANOV, A., CAN, T. & GANESHAN, S. 2018 Odd surface waves in two-dimensional incompressible fluids. *SciPost Physics* **5** (1), 010.
- ASSELIN, O. & YOUNG, W.R. 2020 Penetration of wind-generated near-inertial waves into a turbulent ocean. *Journal of Physical Oceanography* **50** (6), 1699–1716.
- AVRON, J.E. 1998 Odd viscosity. *Journal of Statistical Physics* **92** (3-4), 543–557.
- AVRON, J.E., SEILER, R. & ZOGRAF, P.G. 1995 Viscosity of quantum Hall fluids. *Physical Review Letters* **75** (4), 697.
- BANERJEE, D., SOUSLOV, A., ABANOV, A.G. & VITELLI, V. 2017 Odd viscosity in chiral active fluids. *Nature Communications* **8** (1), 1573.

- BATCHELOR, G. K. 1967 *An introduction to fluid dynamics*. Cambridge: Cambridge University Press.
- BIRE, S., KANG, W., RAMADHAN, A., CAMPIN, J.-M. & MARSHALL, J. 2022 Exploring ocean circulation on icy moons heated from below. *Journal of Geophysical Research: Planets*, **127**, e2021JE007025.
- BUSH, J.W.M., STONE, H.A. & BLOXHAM, J. 1995 Axial drop motion in rotating fluids. *Journal of Fluid Mechanics* **282**, 247–278.
- BUSH, J.W.M., STONE, H.A. & TANZOSH, J.P. 1994 Particle motion in rotating viscous fluids: Historical survey and recent developments. *Current Topics in The Physics of Fluids* **1**, 337–355.
- CHANDRASEKHAR, S. 1961 *Hydrodynamic and hydromagnetic stability*. Oxford University Press.
- DAHLER, J.S. & SCRIVEN, L.E. 1961 Angular momentum of continua. *Nature* **192**, 36–37.
- DAVIDSON, P.A. 2013 *Turbulence in rotating, stratified and electrically conducting fluids*. Cambridge University Press, Cambridge.
- DAVIDSON, P.A. 2014 The dynamics and scaling laws of planetary dynamos driven by inertial waves. *Geophysical Journal International* **198** (3), 1832–1847.
- DAVIDSON, P.A. & RANJAN, A. 2018 On the spatial segregation of helicity by inertial waves in dynamo simulations and planetary cores. *Journal of Fluid Mechanics* **851**, 268–287.
- DRANSFELD, L., DWANE, O. & ZUUR, A.F. 2009 Distribution patterns of ichthyoplankton communities in different ecosystems of the Northeast Atlantic. *Fisheries Oceanography* **18** (6), 470–475.
- FRUCHART, M., SCHEIBNER, C. & VITELLI, V. 2023 Odd viscosity and odd elasticity. *Annual Review of Condensed Matter Physics* **14**, 471–510.
- GANESHAN, S. & ABANOV, A.G. 2017 Odd viscosity in two-dimensional incompressible fluids. *Physical Review Fluids* **2** (9), 094101.
- GAO, F., CHEW, J.W., MARXEN, O. & OTHERS 2020 Inertial waves in turbine rim seal flows. *Physical Review Fluids* **5** (2), 024802.
- GREENSPAN, H.P. 1968 *The theory of rotating fluids*. Cambridge Univ Press.
- KHAIN, T., SCHEIBNER, C., FRUCHART, M. & VITELLI, V. 2022 Stokes flows in three-dimensional fluids with odd and parity-violating viscosities. *Journal of Fluid Mechanics* **934**, A23.
- KIRKINIS, E. 2017 Magnetic torque-induced suppression of van-der-Waals-driven thin liquid film rupture. *Journal of Fluid Mechanics* **813**, 991–1006.
- KIRKINIS, E. 2023 Null-divergence nature of the odd viscous stress for an incompressible liquid. *Physical Review Fluids* **8** (1), 014104.
- KIRKINIS, E. & ANDREEV, A.V. 2019 Odd viscosity-induced stabilization of viscous thin liquid films. *Journal of Fluid Mechanics* **878**, 169–189.
- KIRKINIS, E., MASON, J. & OLVERA DE LA CRUZ, M. 2022 Odd viscosity-induced passivation of Moffatt vortices. *Journal of Fluid Mechanics* **950**, A19.
- KNOBLOCH, E. 2022 Geostrophic turbulence and the formation of large scale structure. In *Mathematical and Computational Models of Flows and Waves in Geophysics*, pp. 1–34. Springer.
- LANDAU, L. D. & LIFSHITZ, E. M. 1987 *Fluid Mechanics. Course of Theoretical Physics, Vol. 6*. Pergamon Press Ltd., London-Paris.
- LIFSHITZ, E. M. & PITAEVSKII, L. P. 1981 *Course of theoretical physics. Vol. 10: Physical Kinetics*. Pergamon Press.
- LONG, R.R. 1953 Steady motion around a symmetrical obstacle moving along the axis of a rotating liquid. *Journal of Atmospheric Sciences* **10** (3), 197–203.
- MARKOVICH, T. & LUBENSKY, T.C. 2021 Odd viscosity in active matter: microscopic origin and 3d effects. *Physical Review Letters* **127** (4), 048001.
- MAXWORTHY, T. 1970 The flow created by a sphere moving along the axis of a rotating, slightly-viscous fluid. *Journal of Fluid Mechanics* **40** (3), 453–479.
- MOFFATT, H.K. 1969 The degree of knottedness of tangled vortex lines. *Journal of Fluid Mechanics* **35** (1), 117–129.
- MOFFATT, H.K. 1970 Dynamo action associated with random inertial waves in a rotating conducting fluid. *Journal of Fluid Mechanics* **44** (4), 705–719.

- MOORE, D.W. & SAFFMAN, P.G. 1968 The rise of a body through a rotating fluid in a container of finite length. *Journal of Fluid Mechanics* **31** (4), 635–642.
- OGILVIE, G.I. 2013 Tides in rotating barotropic fluid bodies: the contribution of inertial waves and the role of internal structure. *Monthly Notices of the Royal Astronomical Society* **429** (1), 613–632.
- RINALDI, C. 2002 Continuum modeling of polarizable systems. PhD thesis, Massachusetts Institute of Technology.
- SCHWALBACH, E.J., DAVIS, S.H., VOORHEES, P.W., WARREN, J.A. & WHEELER, D. 2012 Stability and topological transformations of liquid droplets on vapor-liquid-solid nanowires. *Journal of Applied Physics* **111** (2), 024302.
- SONI, V., BILLIGN, E.S., MAGKIRIADOU, S., SACANNA, S., BAROLO, D., SHELLEY, M.J. & IRVINE, W.T.M. 2019 The odd free surface flows of a colloidal chiral fluid. *Nature Physics* **15** (11), 1188–1194.
- SOUSLOV, A., DASBISWAS, K., FRUCHART, M., VAIKUNTANATHAN, S. & VITELLI, V. 2019 Topological waves in fluids with odd viscosity. *Physical Review Letters* **122** (12), 128001.
- TANZOSH, J.P. & STONE, H.A. 1994 Motion of a rigid particle in a rotating viscous flow: an integral equation approach. *Journal of Fluid Mechanics* **275**, 225–256.
- TRITTON, D.J. 1988 *Physical Fluid Dynamics*. Oxford University Press: Oxford.
- TRUESDELL, C. & NOLL, W. 1992 *The nonlinear field theories of mechanics*, 2nd edn. Berlin: Springer-Verlag.
- WHITHAM, G.B. 1974 *Linear and Nonlinear Waves*. Wiley, NY.
- YIH, C.-S. 1959 Effects of gravitational or electromagnetic fields on fluid motion. *Quarterly of Applied Mathematics* **16** (4), 409–415.
- YIH, C.-S. 1988 *Fluid Mechanics*. West River Press, Ann Arbor MI.